Technical Document 1487
March 1989

Technology and Application of Indium Phosphide and Related Semiconductors

A. K. Nedoluha

NAVAL OCEAN SYSTEMS CENTER

San Diego, California 92152-5000

E. G. SCHWEIZER, CAPT, USN
Commander

R. M. HILLYER
Technical Director

ADMINISTRATIVE INFORMATION

This work was performed by Alfred K. Nedoluha, Electronic Material Sciences Division, Code 56, Naval Ocean Systems Center (NOSC).

Released under authority of
H. E. Rast
Electronic Material Sciences Division

FS

REPORT DOCUMENTATION PAGE

1a. REPORT SECURITY CLASSIFICATION UNCLASSIFIED	1b. RESTRICTIVE MARKINGS
2a. SECURITY CLASSIFICATION AUTHORITY	3. DISTRIBUTION/AVAILABILITY OF REPORT Approved for public release; distribution is unlimited.
2b. DECLASSIFICATION/DOWNGRADING SCHEDULE	
4. PERFORMING ORGANIZATION REPORT NUMBER(S) NOSC TD 1487	5. MONITORING ORGANIZATION REPORT NUMBER(S)
6a. NAME OF PERFORMING ORGANIZATION Naval Ocean Systems Center 6b. OFFICE SYMBOL (If applicable) NOSC	7a. NAME OF MONITORING ORGANIZATION
6c. ADDRESS (City, State and ZIP Code) San Diego, CA 92152-5000	7b. ADDRESS (City, State and ZIP Code)
8a. NAME OF FUNDING/SPONSORING ORGANIZATION Naval Ocean Systems Center 8b. OFFICE SYMBOL (If applicable)	9. PROCUREMENT INSTRUMENT IDENTIFICATION NUMBER
8c. ADDRESS (City, State and ZIP Code) San Diego, CA 92152-5000	10. SOURCE OF FUNDING NUMBERS PROGRAM ELEMENT NO.: In-house PROJECT NO. TASK NO. AGENCY ACCESSION NO.

11. TITLE (include Security Classification)

TECHNOLOGY AND APPLICATION OF INDIUM PHOSPHIDE AND RELATED SEMICONDUCTORS

12. PERSONAL AUTHOR(S)

A. K. Nedoluha

13a. TYPE OF REPORT	13b. TIME COVERED	14. DATE OF REPORT (Year, Month, Day)	15. PAGE COUNT
Final	FROM TO	March 1989	95

16. SUPPLEMENTARY NOTATION

17. COSATI CODES			18. SUBJECT TERMS (Continue on reverse if necessary and identify by block number)
FIELD	GROUP	SUB-GROUP	semiconductor technologies quantum wells diodes

19. ABSTRACT (Continue on reverse if necessary and identify by block number)

This document presents a comprehensive survey of the literature of InP and related III-V compound semiconductors. It identifies the areas where these materials could make an impact on device technology.

20 DISTRIBUTION/AVAILABILITY OF ABSTRACT	21. ABSTRACT SECURITY CLASSIFICATION
☐ UNCLASSIFIED/UNLIMITED ☒ SAME AS RPT ☐ DTIC USERS	UNCLASSIFIED

22a. NAME OF RESPONSIBLE PERSON	22b. TELEPHONE (include Area Code)	22c. OFFICE SYMBOL
A. K. Nedoluha	(619) 553-1032	Code 56

DD FORM 1473, 84 JAN

83 APR EDITION MAY BE USED UNTIL EXHAUSTED
ALL OTHER EDITIONS ARE OBSOLETE

Table of Contents

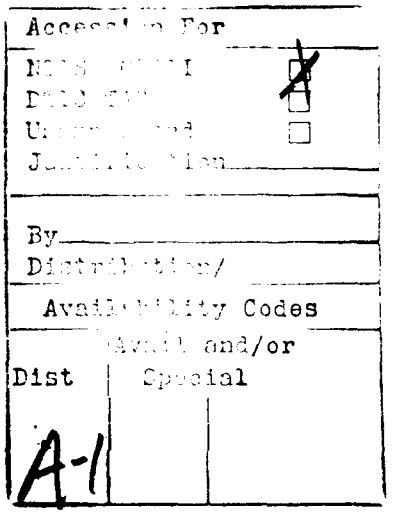

FOREWORD

Immediately prior to his retirement, Dr. Alfred K. Nedoluha completed a comprehensive survey of the literature of InP and related III-V compound semiconductors. His purpose was to identify the areas where these materials could make an impact on device technology. This technical document is the result.

To assist the reader, a glossary has been added. Workers in this field tend to be very liberal in their use of acronyms and abbreviations.

Only a few figures have been included. Readers who wish more details will, of course, have to consult the original publications. Dr. Nedoluha did not intend to produce a review paper, but rather a "white paper", condensed and terse, but broad in scope.

The material included covers the field only to January 1988. Since that time, the literature has significantly expanded and new results are being reported almost daily. Nevertheless, it is hoped that the reader will find this to be a useful document.

H. E. RAST, JR., Head
Electronic Material Sciences Division
Naval Ocean Systems Center

EXECUTIVE SUMMARY

SEMICONDUCTOR TECHNOLOGIES

Si

Silicon technology, the most mature, has the advantage of being based on an inexpensive, elemental and abundant material whose oxide, SiO_2, represents one of the best and most easily grown. The disadvantage of silicon is its indirect bandgap which does not allow the efficient electron-hole recombination required for conventional photoemitters. This indirect gap is accompanied by a large electron effective mass, and hence low mobility, which limits the speed of Si devices.

III-V

The III-V compound semiconductors, under consideration, offer the advantage over silicon of a direct bandgap, which gives high electron mobility and peak velocity and provides strong luminescence which allows photonic applications. A further advantage is their subsidiary conduction band minima which produce negative differential resistivity enabling the production of mm-wave diodes. Finally, heteroepitaxy of III-V materials permits the construction of quantum-well (QW) structures. These advantages represent unique capabilities for indium phosphide (InP) and gallium arsenide (GaAs) with respect to silicon. Because these advantages are shared by both compounds, the competition between InP and GaAs extends over the whole range of electronics and photonics.

InP

Virtually every aspect of III-V compound material and device development has first been demonstrated or attempted on GaAs and then repeated on InP. This is connected to the fact that the first GaAs integrated circuits were demonstrated about 35 years ago and that the capital and labor investment in GaAs technology is at least an order of magnitude larger than that for InP. Nevertheless, InP devices usually outperform their GaAs counterparts wherever equivalent structures exist. InP is superior to GaAs in its electron peak velocity, negative differential

resistivity, immunity to side gating, radiation hardness and thermal conductivity.

Alloys

For lattice matched structures, InP includes the ternary alloys InGaAs and InAlAs and the quaternary InGaAsP, while GaAs is most frequently combined with the ternary alloy AlGaAs. Perhaps the most important indium alloy is InGaAs. Due to its small direct bandgap and consequent small effective electron mass, InGaAs has the highest electron velocity for low electric fields of all the materials thus far mentioned. This is coupled with a high peak velocity at a low threshold field, a consequence of the large electron mobility and the large energy difference between the gamma and L conduction band minima in InGaAs. These properties make InGaAs the most promising material for high speed applications at low electric fields. Finally, the bandgap of InGaAs lattice matched to InP allows detection of 1.55 micron radiation.

DOMINANT TECHNOLOGY ISSUES

Growth

In InP technology, techniques for growing bulk InP must be improved to provide higher quality starting material for direct ion implantation and for epitaxial growth. Following leads in bulk GaAs growth, some improvements are now in progress, including the addition of magnetic fields to the liquid encapsulated Czochralski (LEC) method, the vertical gradient freeze method and other techniques. In epitaxy, both metalorganic chemical vapor deposition (MOCVD) and molecular beam epitaxy deposition (MOCVD) and molecular beam epitaxy (MBE) allow the growth of high quality InP based materials with abrupt heterojunctions, but further improvements in epitaxial methods are also needed. Pseudomorphic growth is of scientific and technical significance, but the possibilities of InP-on-Si or InP-on-GaAs should not be used as an excuse for the neglect of further development of InP substrates.

Surfaces

The principal difference between the GaAs and InP surfaces is in native defects which pin the surface Fermi level near the center of the bandgap in GaAs, while it is located near the conduction band edge in InP. This situation has allowed the development of the metal-semiconductor field effect transistor (MESFET) technology to its present advanced state in GaAs, while the practicality of an insulated gate technology for GaAs has yet to be demonstrated. For InP the situation is just the reverse: the position of the surface Fermi level, coupled with a moderately low density of surface defects, allows an insulated gate technology, but seriously limits the practicality of Schottky barriers on n-type material.

Drift

A persistent problem with InP based metal-insulator-semiconductor field effect transistors (MISFETs) has been the electrical instability, or current drift, which will require serious basic research into its causes or prudent choice of applications for its avoidance. For digital circuits and charge coupled devices, the noise margin can be chosen large enough that drift is not a problem. For power MISFETs, the applied radio frequency (RF) gate bias alleviates current drift; in continuous operation an initial power output of 1.5 W was stable within 2% during a 167 hour experiment.

Radiation

The radiation hardness of these technologies increases in the following order; silicon MISFETs, GaAs MESFETs, GaAs junction FETs (JFETs) and InP JFETs. InP substrates and solar cells are harder than their GaAs counterparts. This suggests that serious consideration be given to radiation hard InP junction field effect transistor (JFET) integrated circuits.

ELECTRICAL DEVICES

InP MISFETs, charge coupled devices, and digital enhancement-depletion integrated circuits have been demonstrated by Naval Ocean Systems Center (NOSC) and others and proven superior in speed compared to

MISFETs

GaAs MESFET components of the same dimension. InP power MISFETs have demonstrated power outputs per unit gate width of up to 4.5 W/mm, more than three times that reported for GaAs.

Gunn

InP Gunn diodes have been demonstrated up to 140 GHz, with operation expected as high as 200 GHz, more than twice as high as for GaAs. A 50 mW InP Gunn amplifier operating between 75-110 GHz has been developed by Varian and the Naval Ocean Systems Center (NOSC). Oscillations have been observed at NOSC in surface-oriented InP Gunn diodes capable of monolithic integration.

HJ

Heterojunction (HJ) devices are being developed to avoid surface Fermi level pinning and provide low scattering interfaces for high channel mobilities. These include the heterojunction insulated gate field effect transistor (HIGFET) and the modulation-doped FET. Promising InGaAs/InAlAs heterojunction insulated gate FETs have been reported, and a device with an InP channel and an InGaAs insulator has been demonstrated jointly by University of California, San Diego (UCSD) and NOSC.

DBRT

An interesting device element for ultra-high speed applications is the double-barrier resonant-tunneling (DBRT) diode. For a pseudomorphic AlAs/InGaAs diode on InP, a peak-to-valley ratio of 14 has been achieved in the negative differential resistance at room temperature. This should be compared to the ratio of 4 for the best AlGaAs/GaAs DBRT diode. DBRT diodes provide a convenient way of making three-state memory cells for integrated circuits using multiple-valued logic.

OPTICAL DEVICES

The photonics area is dominated by the rapid progress made in laser diode (LD) technology. The following achievements have been reported for room temperature continuous operation in the 1.3 to 1.55 μm wavelength region: a laser diode with a 3 db bandwidth of 22

GHz, a distributed feedback laser with a single longitudinal mode output power of 52 mW, a surface emitting laser diode array with a flux of 57 W/cm^2, and the first quantum well laser diode involving wells sufficiently thin to exhibit two dimensional excitons. Stimulated light emission from quantum boxes by current injection at 77^oK was observed for the first time. The possibility of room temperature operation without distributed feedback or external cavities has been suggested by the recent report of a rare earth (RE) doped semiconductor laser diode.

Lasers

InGaAs/InAlAs optoelectric intensity modulators using multiple quantum-wells have shown superior performance to Franz-Keldysh modulators and to similar structures made from the AlGaAs/GaAs system. InGaAs/InP multiple quantum-well (MQW) modulators are being developed by NOSC.

Modulators

InGaAs/InAlAs p-i-n photodiodes have been demonstrated with a 3 db bandwidth of 18 GHz.

Detectors

Monolithic optoelectronic integrated circuits (MOICs) offer performance and economic advantages over hybrid circuits but at present do not meet theoretical expectations. Recent developments involving strained-layer structures include InGaAs photodetectors (PD) on GaAs substrates which have been integrated with GaAs MESFETs, GaAs MESFETs on InP substrates integrated with InGaAs detectors, and InGaAs detectors grown on silicon. InP based MOICs have the advantage compared to GaAs of higher speed and a transparent substrate which allows back illumination of the detectors and largely eliminates optical crosstalk between lasers and transistors. The monolithic integration of an InGaAs detector with an InP JFET transimpedance amplifier is being carried out in a cooperative effort between NOSC and the University of Southern California.

MOICs

A variety of novel device functions has been reported. They are based either on the inherent nonlinearity of photonic devices or on nonlinearities

Novel resulting from the interaction of vertically integrated electronic and photonic device structures. Screening by virtual charge carriers promises ultrafast optical nonlinear quantum-well devices.

RECOMMENDATION

InP technology offers the following advantages in military applications: InP MISFETs for power, InP JFETs for radiation hard integrated circuits, InGaAs for speed and InP based electronic and photonic devices for monolithic integration. Broad DoD support is recommended to take advantage of these opportunities.

I. INTRODUCTION

Indium phosphide (InP) and gallium arsenide (GaAs) form the basis for two families of group III-V semiconductor materials with a wide range of electronic and optoelectronic applications. For device structures and monolithic integrated circuits (ICs), GaAs is frequently combined with epitaxial layers of $Al_xGa_{1-x}As$, and InP with $In_xGa_{1-x}As_yP_{1-y}$ or $In_xAl_{1-x}As$. An important special case of the quaternary alloy InGaAsP (we shall commonly omit the composition indices x and y) is the ternary InGaAs, usually grown on InP, but lately in the form of pseudomorphic layers also on GaAs. This paper deals primarily with the technology and applications of indium compounds and alloys on InP, with information on other materials, in particular GaAs, provided for comparison.

The status of InP technology is generally far below that of GaAs, which again is immature compared to that of silicon (Si). With exception of applications to photoemitters and photodetectors for fiber optic (FO) communications, the commercial incentive for industrial development of GaAs and InP technology has been relatively low. The high performance III-V semiconductor monolithic integrated circuit (IC) technology is primarily driven by military requirements (I.1). Consequently, Defense Advanced Research Projects Agency (DARPA) has provided financial support to industry to establish pilot production lines for GaAs digital circuits, and Office of Undersecretary Defense (Research & Advanced Technology) has initiated the Microwave/Millimeterwave Monolithic Integrated Circuit (MIMIC) program. The baseline technology is GaAs submicron metal-semiconductor field effect transistors (MESFETs) for MIMIC, and MESFETs or junction field effect transistors (JFETs) for the DARPA digital circuits.

Another technology which has received a fair amount of support from DARPA and other DOD sources is that of $Hg_xCd_{1-x}Te$ and related II-VI compounds and alloys for infrared (IR) detectors and focal plane arrays (FPAs). HgCdTe offers the advantage that it can cover both of the atmospheric windows of 3 - 5 and of 8 - 14 micrometer. It has the disadvantage that the technology of II-VI materials is considerably more difficult than that of III-V materials. The short wavelength window as well as a portion of the long wavelength window are within the range of III-V materials either grown lattice matched or as strained-layers; for

InAsSb on indium arsenide (InAs) substrates a cut-off wavelength of 12.5 μm has been obtained (I.2). DOD's recent Infrared Focal Plane Array (IRFPA) Producibility Initiative will address both HgCdTe and InSb.

Financial support for the development of other semiconductor technologies (with exception of Si, of course), has been on a relatively low level. The largest systematic support to develop an InP based technology was a Special Technology Program funded by Office of Naval Technology (ONT); this program terminated at the end of FY86. As indicated in the following, InP based technology offers a wide range of unique opportunities well deserving a major initiative.

The approach taken in this report is to compare advantages and disadvantages of various technologies and device developments, quote review papers where available, and supplement these by newly published results. A review of semiconductor optoelectronics efforts toward high speed operation has been given by Kao (I.3).

I.1: Analysis, Commentary and Recommendations, AGED Working Group B (Microelectronics), Special Technology Area Review (STAR) on Monolithic GaAs IC System Application and Insertion, GED-L 80/84-9, Oct 1984

I.2: M. Y. Yen, B. F. Levine, C. G. Bethea, K. K. Choi, and A. Y. Cho, Appl. Phys. Lett. 50 (1987) 927

I.3: C. K. Kao, IEE Proc. 133 Pt. J (1986) 230

II. MATERIAL PROPERTIES AND QUANTUM-WELLS

The bandgaps and lattice constants of various III-V compounds and ternary alloys are shown in Figure 1. For the electronically active regions of III-V semiconductor structures the most important materials are GaAs, InP, InGaAs, and InGaAsP. The quaternary alloy InGaAsP can be lattice matched either to GaAs or InP, but its most prominent role is that in optoelectronics, lattice matched to InP. Adding a fifth element to obtain alloys such as AlInGaAsP increases flexibility for desired material

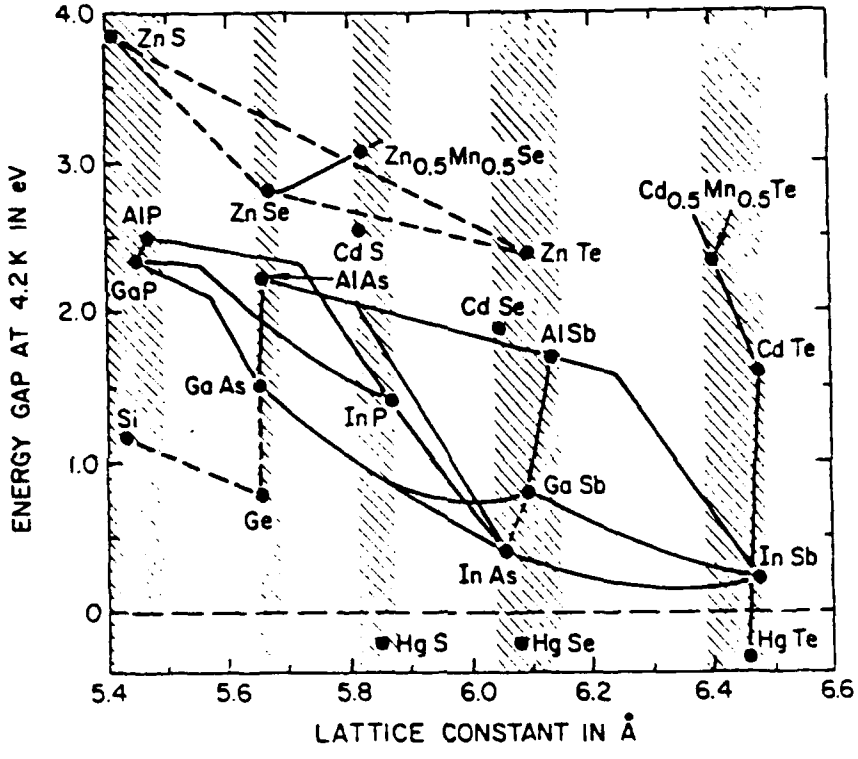

Figure 1. Energy gaps at 4.2°K versus lattice constants, from reference II,C.1.

parameters but little work has been reported so far on pentanaries (II.1). Characteristic properties of GaAs, InP, and of $In_xGa_{1-x}As$ lattice matched to InP, corresponding to x = 0.53, are given in Table I.

II.1: K. Asami, T. Okuno, S. Emura, S. Gonda, and S. Mukai, Appl. Phys. Lett 51 (1987) 1720

II.A. Optical and Transport Properties

The materials in Table I, as well as InGaAsP, have direct bandgaps with strong interband luminescence near the bandgap wavelength and strong absorption at shorter wavelengths which makes them useful in photonics and optoelectronics. The bandgap of GaAs happens to fall in the short wavelength window of silica fibers which makes GaAs the appropriate photoemitter material for short wavelength near infrared (NIR) fiber optics (FO). InGaAs lattice matched to InP has a bandgap appropriate for photodetection in long wavelength NIR FO. Proper choice of the compositions x and y in $In_xGa_{1-x}As_yP_{1-y}$ allows lattice matching to InP and, simultaneously, to choose a desired bandgap between that of InP and InGaAs, which makes InGaAsP an appropriate photoemitter alloy for long wavelength NIR FO.

After considerable controversy on the band offsets in heterojunctions, particularly for AlGaAs/GaAs, some consensus seems to have developed. The approximate ratios of the conduction band offsets to the valence band offsets are 62:38 for AlGaAs/GaAs (II,A.1), 42:58 for $InP/In_{0.53}Ga_{0.47}As$ (II,A.2), and 70:30 for $In_{0.52}Al_{0.48}As/In_{0.53}Ga_{0.47}As$ (II,A.3).

Figure 2 compares the steady state electron drift velocities versus electric field for Si, GaAs, InP, and InGaAs. The III-V materials exhibit a maximum in the velocity-field characteristics caused by the transfer of conduction electrons from the Gamma minimum to higher subsidiary minima at sufficiently high electric fields. The electric field at the maximum is the threshold field for the onset of negative differential resistance (NDR). Due to

Table I. Comparison of Material Properties at 300°K

Type Material:		InP	GaAs	InGaAs
Bandgap energy	eV	1.34	1.43	0.75
Gamma-L energy diff.	eV	0.6	0.36	0.55
Electron relative eff. mass at Gamma		0.08	0.07	0.04
Low field electron mob. for high purity	cm^2/Vs	5000	8000	12000
for 10^{17} donors/cm^3	cm^2/Vs	3000	5000	10000
Threshold field	kV/cm	12	3.6	3
Peak electron veloc.	10^7 cm/s	2.2	1.7	2.8
Saturated el. veloc.	10^7 cm/s	0.8	0.7	0.6
Peak-to-valley electron velocity ratio		3 - 4	2 - 2.5	4 - 5
Threshold energy for impact ionization by electrons	eV	2.1	1.7	low?
Electric field for alpha = 10^4 cm^{-1}	kV/cm	530	390	low?
Thermal conductivity	W/cm-K	0.7	0.5	0.06
Native surface donor energy below CBM	eV	0.1	0.9	0.25?
Native surface acceptor energy below CBM	eV	0.5	0.7	0.25?

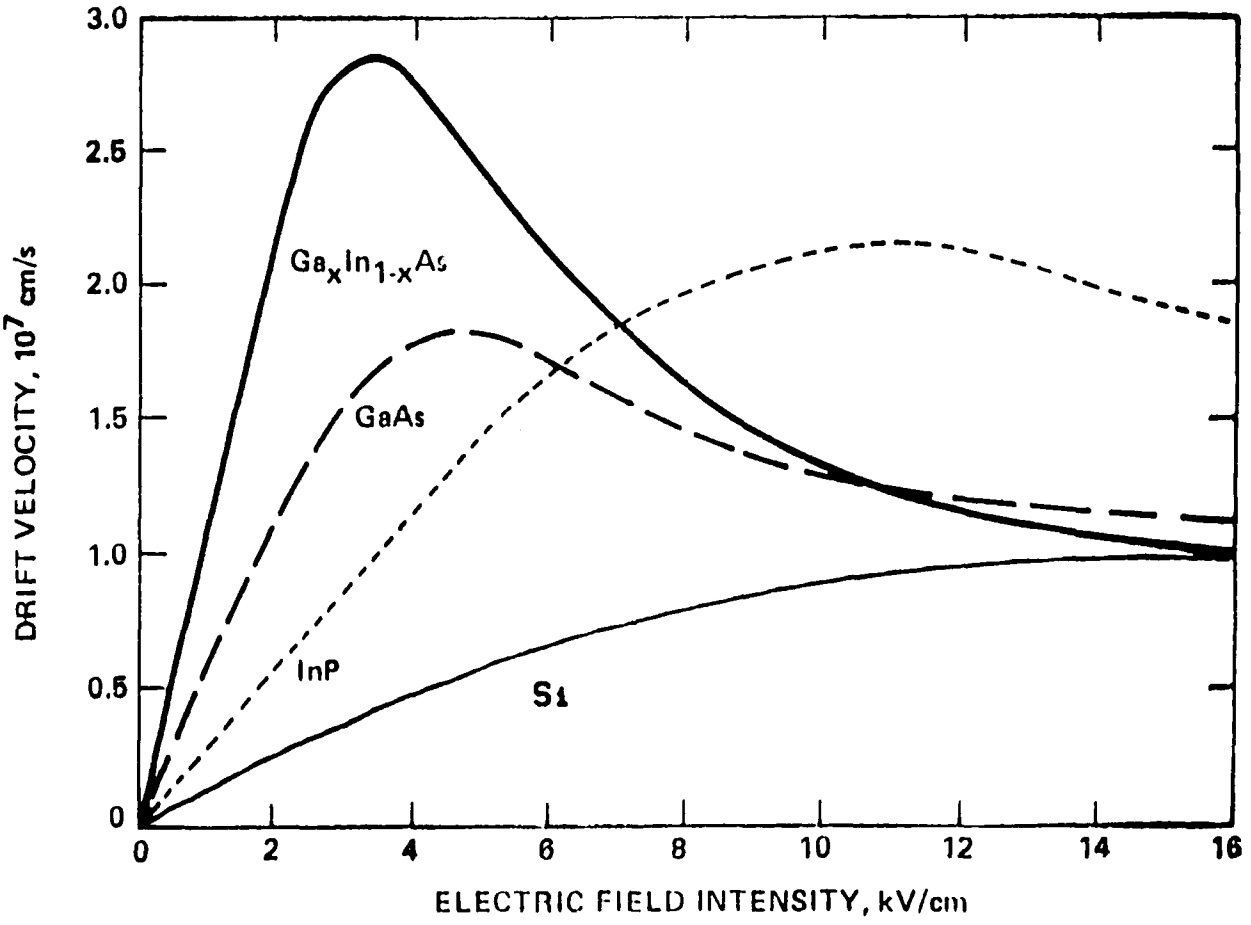

Figure 2. Electron drift velocities versus applied electric field.

its small direct bandgap and consequent small effective electron mass, InGaAs has the highest electron velocity among these materials for low electric fields. This is coupled with a high peak velocity of InGaAs at a low threshold field, consequences of the large electron mobility and the large energy difference between the Gamma and L conduction band minima in InGaAs. These properties make InGaAs the most promising material for high speed and high frequency applications at low electric fields.

For pure III-V materials as used, e.g., for the active layers in modulation doped structures, the electron mobilities at room temperature are limited by optical phonon scattering. Cooling reduces phonon scattering and, therefore, increases the mobilities. In alloys, the random occupation of certain or all lattice sites by different elements produces alloy scattering which may dominate in pure materials at low temperature and makes it less attractive to cool InGaAs (II,A.4).

At higher electric fields, InP has the highest electron drift velocity among the materials compared in Figure 2. The superiority of InP over GaAs shown is due to the larger energy difference between the Gamma and L conduction band minima in InP. High electric fields are desirable for specific applications such as power FETs, but they may also be an unavoidable consequence of the combination of small device size and the necessity of operating with voltages above a certain minimum magnitude such as imposed on digital applications by the maximum allowed bit error rate (BER). For such small structures the situation may become complicated by velocity overshoot as discussed below.

At very high electric fields the electron drift velocities saturate or, for the III-V materials, may first go through a minimum. These high field velocity values are not well known. Approximate values for the electron saturation velocities and the velocity peak-to-valley ratios are given in Table I. The peak-to valley ratios are higher in InP and InGaAs than in GaAs which is of advantage for InP transferred electron devices (TEDs).

The threshold energy for impact ionization by electrons is higher in InP than in GaAs which gives InP a lower electron ionization rate, alpha, for a given electric field. To obtain a certain ionization rate, say alpha = 10^4 cm^{-1}, requires a higher electric

field in InP than in GaAs (see Table I) which can be taken as an indication of higher electric breakdown strength of InP and is clearly desirable for any high field applications.

The velocity and ionization data given above hold for long structures in steady state. For times less than the electron energy relaxation time, the electron velocity for high electric fields may overshoot the steady state saturation velocity (II,A.5), (II,A.6). This velocity overshoot lasts less than a picosecond in Si, but may extend to several picoseconds in GaAs, InP, or InGaAs. For devices with electron transit times less than that, a higher effective saturation velocity results. This occurs for device lengths less than 0.1 μm in Si, while in GaAs or InP velocity overshoot may be observed for several tenths of microns, and for more than 1 μm in InGaAs. The limiting case is that of ballistic transport. A qualitative discussion of ballistic transport is provided in (II,A.7). Impact ionization and avalanching are similarly modified for short devices (II,A.8).

The thermal conductivity of InP is higher than that of GaAs which helps with heat dissipation, but is less than half of the 1.5 W/cm-K of Si.

II,A.1: H. Kroemer, Surface Science 174 (1986) 299

II,A.2: D. V. Lang, M. B. Panish, F. Capasso, J. Allam, R. A. Hamm, A. M. Sergent, and W. T. Tsang, Appl. Phys. Lett. 50 (1987) 736

II,A.3: R. People, K. W. Wecht, K. Alavi, and A. Y. Cho, Appl. Phys. Lett. 43 (1983) 118

II,A.4: Y. Takeda and A. Sasaki, Japan. J. Appl. Phys. 24 (1985) 1307

II,A.5: D. K. Ferry, Adv. Electronics and Electron Physics 58 (1982) 311

II,A.6: B. R. Nag, S. R. Ahmed, and M. D. Roy, IEEE Trans. Electron Devices ED-33 (1986) 788

II,A.7: M. Heiblum and L. F. Eastman, Scientific American, Feb. 1987. p. 102

II,A.8: M. S. Gupta, IEEE Electron Device Lett. EDL-8 (1987) 469

II.B. Defect Related Properties

Native point defects can occur in the bulk and on the surface in the form of vacancies, interstitials, antisite defects, or related complexes. The defect level energy is expected to shift when moving a defect from the bulk towards the surface which makes the correlation of bulk and surface defects non-trivial.

The most important but poorly understood bulk defect in GaAs is the EL2 donor which can pin the Fermi level near the center of the bandgap and make the material semi-insulating. The EL2 level is probably due to a complex consisting of the As_{Ga} antisite defect and either an As_i interstitial (II,B.1) or one or even two V_{As} vacancies (II,B.2). For InP, a deep native bulk acceptor level which can make the material semi-insulating seems to exist both in bulk (II,B.3) and in epitaxial (II,B.4) material, but present evidence is insufficient.

Surface characteristics will depend on intrinsic surface states and on surface defects. For the materials under consideration, intrinsic surface states with energy levels in the bandgap are not expected. This is confirmed by measurements on crystals cleaved in vacuum: for sufficiently low step densities no band bending occurs in the surface region. Exposure to oxygen or deposition of metals, however, produces native surface defects which pin the Fermi level at insulator-semiconductor and metal-semiconductor interfaces (II,B.5). GaAs has deep surface donors and acceptors which confine the surface Fermi level to an energy region in the vicinity of the center of the bandgap and slightly below. InP has shallow surface donors and deep surface acceptors which tend to keep the surface Fermi level in the upper half of the bandgap. For InGaAs, shallow surface defects have been suggested (II,B.6) to pin the surface Fermi level in the upper half of the bandgap (II,B.7). The precise nature of these defects is uncertain. Spicer (II,B.5) has suggested that missing anions (such as the group V elements As or P) give acceptors, and

that missing cations (such as the group III elements Ga or In) give donors. Others have suggested the opposite assignment for defects in InP, and have associated both the native donor and acceptor in GaAs to a missing As atom. In semiconductor-semiconductor junctions with well matched interfaces such native defects occur only in low densities or not at all.

Surface state densities (N_{SS}), observed primarily in semiconductor-insulator structures as U-shaped functions of energy, may be related to the native surface defects in the semiconductor, dangling bonds in the interface, traps in the insulator communicating with the semiconductor by tunneling, or combinations thereof. The N_{SS} densities depend strongly on processing; they have minimum values from low 10^{12} to high 10^{13} $cm^{-2}eV^{-1}$ for GaAs, and may be one or two orders of magnitude less for InP and InGaAs.

The mid bandgap surface Fermi level and high N_{SS} in GaAs leads to high surface recombination velocities, while the surface Fermi levels in the upper half of the bandgaps of InP and InGaAs combined with the lower N_{SS} values give low surface recombination velocities.

Surface electric breakdown in semi-insulating (SI) GaAs seems to be dominated by surface states and gives nominal electric breakdown fields which are one to two orders of magnitude smaller then those for SI InP surfaces (II,B.8).

Radiation can produce native defects. InP bulk crystals show higher tolerance for gamma irradiation than GaAs (II,B.9). For InP JFETs, the total dose hardness level is greater than 10^8 rad for 1 MeV gamma irradiation; for 1 MeV electron irradiation it is greater than 8×10^8 rad, exceeding that of GaAs MESFETs by more than an order of magnitude (II,B.10). InP solar cells have been shown to be more radiation hard than Si or GaAs cells for irradiation with 60_{Co} gamma-rays (II,B.11) or 1 MeV electrons (II,B.12).

II,B.1: C. Song, W. Ge, D. Jiang, and C. Hsu, Appl. Phys. Lett. 50 (1987) 1666

II,B.2: Y.-T. Shen and C. W. Myles, Appl. Phys. Lett. 51 (1987) 2034

II,B.3: C. R. Zeisse, personal communication

II,B.4: M. Sugawara, O. Aoki, N. Nakai, K. Tanaka, A. Yamaguchi, and K. Nakajima in "Semi-Insulating III-V Materials", Omsha, Tokyo, and North-Holland, Amsterdam, 1986, p.597

II,B.5: W. E. Spicer, I. Lindau, P. R. Skeath, and C. Y. Su, Applications of Surface Science 9 (1981) 83

II,B.6: H. H. Wieder, Appl. Phys. Lett. 38 (1981) 170

II,B.7: H. H. Wieder, J. L. Veteran, A. R. Clawson, and D. P. Mullin, Appl. Phys. Lett. 43 (1983) 287

II,B.8: H. Hasegawa, T. Kitagawa, H. Masuda, H. Yano, and H. Ohno, Proc. Symp. Dielectric Films on Compound Semiconductors, edited by V. J. Kapoor, D. C. Connolly, and Y. H. Wong, publ. by Electrochem. Soc., Proc. Vol. 86-3 (1986) 227

II,B.9: M. Kitagawa and K. Nakamura, IEEE Trans. Nuclear Sci. NS-34 (1987) 1704

II,B.10: W. T. Anderson and J. B. Boos, IEEE Trans. Nuclear Sci., NS-32 (1985) 4001

II,B.11: M. Yamaguchi, C. Uemura, and A. Yamamoto, J. Appl. Phys. 55 (1984) 1429

II,B.12: M Yamaguchi, C. Uemura, A. Yamamoto, and A. Shibukawa, Japan. J. Appl. Phys. 23 (1984) 302

II.C. Two Dimensional Electron Gas and Quantum-well Structures

Spatial confinement of electrons and holes in semiconductors to distances of the order of 10 nm or less in one or more dimensions produces quantum size effects which modify certain material properties and allow the engineering of materials with new effective characteristics. A general survey of QW structures and superlattices (SLs) has been presented by Esaki (II,C.1). Surveys

of QW structures with emphasis on photonics have been given by Chemla (II,C.2) and, more recently, by Okamoto (II,C.3).

The two-dimensional electron gas (2-DEG), as it occurs in sufficiently narrow inversion and accumulation layers or in an one-dimensional (1-D) QW, is characterized by a density of states that is no longer parabolic in energy, as for the bulk, but is of a staircase form, with a nonvanishing density of states even at the minimum allowed energy. In a 2-D QW structure, also referred to as quantum wire, the density of states is a saw tooth like function with (in lowest order theory) infinite peaks; for a 3-D QW, also designated as QW box or quantum-dot structure, the density of states becomes a train of delta functions. Recent examples are GaAs quantum wires made by focused ion beam implantation (II,C.4), InGaAs/InP quantum wires and QW boxes by MBE (II,C.5), and InGaAsP/InP QW boxes by MOCVD (II,C.6).

A QW structure with barriers sufficiently thin that charge carriers can tunnel through (tunnel barrier), may show NDR if the applied bias places the energy of the incident carrier in resonance with one of the QW levels (resonant tunneling).

The term "superlattice (SL)" is used either for any periodic multilayer structure or, more specifically, for a periodic multiple-quantum-well (MQW) structure with tunnel barriers (II,C.7) in which case the energy levels in the wells are broadened to SL minibands.

In type I SLs such as GaAs wells between AlGaAs barriers, InGaAs wells between InP or InAlAs barriers, or strained InGaAs between GaAs barriers (II,C.8) not only the electron gas but the hole gas is quantized within the wells. The staircase shaped density of electron and hole states in the quantum-wells gives significant performance advantages for electronic and photonic applications. Three other kinds of compositional SLs can be distinguished:InAlAs/InP forms a type II-staggered superlattice with electron confinement in InP and hole confinement in InAlAs; GaSb/InAs represents a type II-misaligned SL, with electron confinement in InAs and hole confinement in GaSb, but with the valence band edge of GaSb above the conduction band edge of InAs; in type III SLs, such as HgTe-CdTe, one constituent is a semi-metal.

Two-dimensional (2-D) excitons in type I QW structures, for the limit of infinitely high barriers, have ionization energies four times and oscillator strengths eight times those of the three-dimensional (3-D) bulk excitons. The 2-D excitons remain dominant features at room temperature, where 3-D excitons are negligible, and have been observed in InGaAs/InP QWs up to 450^{o}K (II,C.9). Absorption saturation (bleaching) due to exciton quenching caused by phase space filling and screening of the 2-D excitons by free carriers represents an optical non-linearity much stronger than that in bulk material and can give optical bistability for light intensities much lower than in the bulk. Absorption coefficient and index of refraction are affected by free carriers, band gap renormalization due to many body effects, and by Burstein-Moss shift due to band filling (II,C.7). Optical nonlinearities are even stronger in asymmetric coupled QWs, i.e., QWs of unequal width separated by a narrow tunnel barrier (II,C.10).

Optical nonlinearity of exciton absorption is not confined to the presence of real charge carriers. For optical pumping below the absorption edge, a blue shift and bleaching of exciton absorption has been observed (II,C.11), (II,C.12), caused by the optical Stark effect (II,C.13), i.e., the effect of the electric field of the nonresonant pump beam.

Application of a static (or quasi-static) electric field across the QW leads to the quantum confined Stark effect (QCSE) observed in luminescence and absorption. The 2-D exciton peaks decrease in intensity, shift to longer wavelengths, and broaden with increasing electric field; optical transitions forbidden for zero field become allowed. The confinement by the barriers prevents dissociation of the 2-D excitons even at fields of 100 kV/cm. The QCSE in QW structures is much more efficient for optoelectronic light modulation than electroabsorption (Franz-Keldysh effect) in the bulk.

For biased QWs, blue shift and exciton bleaching by optical pumping below the absorption edge has recently been proposed due to screening of the applied electric bias field by virtual electrons and holes (II,C.14), (II,C.15). Mechanisms which do not depend on the creation and removal of real charge carriers are expected to allow much higher modulation or switching speeds.

MQWs and SLs serve in at least four functions: (1) to enhance quantum effects obtainable from a single quantum-well (SQW); (2) as superalloys (II,C.16), e. g., as an alternative to random alloys, by displaying effective material characteristics which are some average of the well and barrier material properties, except that these structures are anisotropic; (3) as the starting material for alloy formation by compositional disordering (see Sec.III.C); (4) to act as buffer layers, based on the property of pseudomorphic SLs that dislocations entering from the substrate have a tendency to bend parallel to the SL interfaces and, therefore, will not penetrate into the active material.

Strained-layer superlattices (SLSs) provide further flexibility in tailoring material properties and offer new material features for device applications. Brief reviews have been given by Osbourn (II,C.17), (II,C.18).

All of the above SLs are of the compositional type. A different kind of SL is the n-i-p-i crystal or doping SL, consisting of a periodic repetition of n and p-type doped regions with optional undoped (intrinsic) regions in between. This results in physical separation of the confinement regions for electrons and holes, similar to type II SLs. A review of n-i-p-i structures and potential applications has been given by Dohler (II,C.19). Optical nonlinearity for absorption by an InP n-i-p-i SL at 77^{o}K has been reported (II,C.20) for light intensities at least one order of magnitude smaller than for GaAs MQW structures. Combining compositional and doping periodicity results in hetero n-i-p-i SLs, of interest for photonic devices.

II,C.1: L. Esaki, IEEE J. Quantum Electron. QE-22 (1986) 1611

II,C.2: D. S. Chemla, Physics Today, May 1985, p. 57

II,C.3: H. Okamoto, Japan. J. Appl. Phys. 26 (1987) 315

II,C.4: T. Hiramoto, K. Hirakawa, Y. Iye, and T. Ikoma, Appl. Phys. Lett. 51 (1987) 1620

II,C.5: H. Temkin, G. J. Dolan, M. B. Panish, and S. N. G. Chu, Appl. Phys. Lett. 50 (1987) 413

II,C.6: Y. Miyamoto, M. Cao, Y. Shingai, K. Furuya, Y. Suematsu, K. G. Ravikumar, and S. Arai, Japan. J. Appl. Phys. 26(1987) L225

II,C.7: D. S. Chemla and D. A. B. Miller, J. Opt. Soc. Am. B 2 (1985) 1155

II,C.8: I. J. Fritz, J. E. Schirber, E. D. Jones, T. J. Drummond, and L. R. Dawson, Appl. Phys. Lett. 50 (1987) 1370

II,C.9: Y. Kawaguchi and H. Asahi, Appl. Phys. Lett. 50 (1987) 1243

II,C.10: J. W. Little, J. K. Whisnant, R. P. Leavitt, and R. A. Wilson, Appl. Phys. Lett. 51 (1987) 1786

II,C.11: A. Mysyrowicz, D. Hulin, A. Antonetti, A. Migus, W. T. Masselink, and H. Morkoc, Phys. Rev. Lett. 56 (1986), p. 2748

II,C.12: A. Von Lehmen, D. S. Chemla, J. E. Zucker, and J. P. Heritage, Optics Lett. 11 (1986) 609

II,C.13: S. Schmitt-Rink and D. S. Chemla, Phys. Rev. Lett. 57 (1986) 2752

II,C.14: M. Yamanishi, Phys. Rev. Lett. 59 (1987) 1014

II,C.15: D. S. Chemla, D. A. B. Miller, and S. Schmitt-Rink, Phys. Rev. Lett. 59 (1987) 1018

II,C.16: B. T. McDermott, N. A. El-Masry, M. A. Tischler, and S. M. Bedair, Appl. Phys. Lett. 51 (1987) 1830

II,C.17: G. C. Osbourn, IEEE J. Quantum Electron. QE-22 (1986) 1677

II,C.18: G. C. Osbourn, J. Vac. Sci. Technol. B 4 (1986) 1423

II,C.19: G. H. Dohler, IEEE J. Quantum Electron. QE-22 (1986) 1682

II,C.20.: H. Kobayashi, Y. Yamauchi, H. Kawaguchi, and K. Takahei, Japan. J. Appl. Phys. 25 (1986) L804

III. MATERIAL TECHNOLOGY AND PROCESSING

Devices can be made either directly on the substrate, e.g., enhancement metal-insulator-semiconductor field effect transistors (MISFETs) on SI InP, by ion implantation or diffusion of dopants, by growth of epilayers, or by combinations thereof. We shall discuss substrates, epitaxy and heterojunctions, ion implantation and diffusion, insulators, Schottky barriers and ohmic contacts, and etching.

A brief discussion of materials and processing issues in III-V semiconductors has recently been given by Lester and Streetman (III.1). For an earlier review comparing InP and GaAs and their electronic applications see Wieder (III.2).

III.1: S. D. Lester and B. G. Streetman, Superlattices and Microstructures, 2 (1986) 33

III.2: H. H. Wieder, J. Vac. Sci. Technol. 18 (1981) 827

III.A. Substrates

Bulk InP and GaAs are the usual substrate materials for the two families of semiconductors under discussion. These substrates are available in n-type, p-type, and SI form and are commonly grown by LEC techniques with dislocation densities of 10^4 - 10^5 cm^{-2}; also, InP can show dislocation cluster densities (grappes) of 10^2 - 10^3 cm^{-2} which may be prevented by minimizing the moisture content of the B_2O_3 encapsulant used in the LEC growth of InP (III,A.1).

Crystacomm Inc. is the only commercial U.S. source for InP substrates. (100) oriented InP is available as 2-inch wafers, compared to the usual GaAs 3-inch and recently available 4-inch (III,A.2) wafers. A Navy Manufacturing Technology Program for InP substrate material has been proposed and is under consideration for funding.

For GaAs, the deep levels required to make the material semi-insulating were originally introduced by chromium (Cr) doping which gives a deep acceptor level. Presently, particularly in the U.S., nominally undoped SI GaAs is preferred with the EL2 level introduced as a consequence of the arsenic (As) excess during LEC growth. For SI InP, the preferred dopant is Fe which acts as deep acceptor. SI InP and GaAs are actually weakly n-type with carrier concentrations of the order of 10^8 cm^{-3} or less at room temperature.

Approaches to reduce defect densities include heavy doping (alloying), annealing, application of magnetic fields as in the magnetic liquid-encapsulated Czochralski (MLEC) growth, and the vertical gradient freeze (VGF) technique.

For GaAs, alloying with In hardens the material and can reduce etch pit densities (EPD) due to dislocations by an order of magnitude. For InP, a similar effect can be achieved by heavy doping with S or certain other elements; the resulting strongly n-type material can be used for devices such as photoemitters or, after epitaxial deposition of a SI InP or InAlAs layer, as a low defect substrate for monolithic integration (III,A.3). Nearly dislocation free LEC SI Fe-doped InP has been obtained by hardening the material through co-doping with Ga + Sb (III,A.4). Present Naval Research Laboratory (NRL) efforts aim at lowering the Fe concentration in SI InP.

A comparison of various SI GaAs substrates for low-noise microwave amplifiers has shown whole-ingot annealed high-pressure LEC to give the best noise figure (III,A.5).

MLEC of undoped InP has resulted in an EPD of 6×10^3 cm^{-2} and absence of dislocation clusters (III,A.6). MLEC of S doped InP, co-doped with Ga + Sb, gave dislocation free material.

The VGF technique (III,A.7) can reduce etch pitch densities (EPDs) by an order of magnitude or more and decrease impurity clustering. Improved uniformity of the threshold voltage of GaAs MESFETs on such material has been demonstrated (III,A.8).

VGF and most commercial LEC methods for InP are two-step growth techniques which increase costs and introduce impurities. A new

one-step approach, liquid phosphorus encapsulated Czochralski (LPCZ) growth, has been demonstrated (III,A.9).

Attempts to make utilizable undoped SI InP have not been successful so far. Lightly Zn doped bulk InP seems to have a tendency to SI behavior (II,B.3) but this form of the material is thermally unstable. Since the Zn impurity is a shallow acceptor and not expected to have any deep levels, the SI behavior may be due to a deep native defect in InP caused by the introduction of the Zn impurity. The occurrence of such a native deep level in InP, analog to EL2 in GaAs, would not be unexpected: both GaAs and InP are known to have native surface defect levels (II,B.5) and the bulk GaAs EL2 level may be related to the GaAs native deep surface donor; similarly, the existing native deep surface acceptor in InP suggests the existence of a related native deep bulk acceptor.

To take advantage of the available large size (up to 6-inch or even 8-inch diameter), excellent mechanical properties, high thermal conductivity, and relatively low price of Si substrate wafers, the growth of GaAs on Si is under development in spite of the 4% lattice mismatch of Si and GaAs. Growth techniques such as MBE (III,A.10), migration-enhanced epitaxy (MEE/MBE) (III,A.11), MOCVD with strained-layer superlattices (SLSs) (III,A.12) and other methods are applied (a brief discussion of the various epitaxial growth techniques will be given in the next Section). Whether this is a practical approach to GaAs ICs remains to be seen (III,A.13), but at least it may permit monolithic integration of GaAs components, such as photoemitters for chip-to-chip data transfer, with Si ICs. An interesting variation is the growth of GaAs on silicon-on-sapphire (SOS) substrates (III,A.14). For GaAs/Si monolithic microwave integrated circuits (MMICs) the main concerns are the quality of the active GaAs layer and the preservation of the high resistivity of the Si substrate during GaAs growth (III,A.15).

To take advantage of the advanced GaAs IC technology, the growth of InP and InGaAs photonic devices on GaAs substrates is pursued for monolithic integrated optoelectronic circuit (MIOC) applications. In spite of the 4% lattice mismatch, good InGaAs photoconductors (III,A.16) and InGaAs/InP photodiodes (III,A.17) have been grown on GaAs by MOCVD. Photodiodes with a strained-layer superlattice between the active $In_xGa_{1-x}As$ and the GaAs

substrate have been made by MOCVD for x up to 0.35 (III,A.18). The inverse approach, growth of GaAs and AlGaAs for electronic devices on InP substrates, has also been demonstrated (III,A.19), (III,A.20).

Growth of InP on Si is more difficult because of the 8% lattice mismatch. Growth by MOCVD with (III,A.21) or without (III,A.22) an intermediate GaAs layer, and growth by molecular/ion beam epitaxy (MIBE) with a compositionally graded layer (III,A.23) has been reported. $In_xGa_{1-x}As$ on Si has been grown by MOCVD for x = 0.54 in two steps by first growing GaAs over AlAs/GaAs and $In_{0.1}Ga_{0.9}As$/GaAs superlattices (III,A.24), or directly by MBE for x = 0 to 0.49 (III,A.25).

Attempts to grow homogeneous bulk InGaAs or InGaAsP have not been successful.

III,A.1: B. Cockayne, G. T. Brown, and W. R. MacEwan, J. Cryst. Growth 64 (1983) 48

III,A.2: III-V Technology Review, Vol. II, No. 3 (1987) 18

III,A.3: J. Cheng, R. Stall, S. R. Forrest, J. Long, C. L. Cheng, G. Guth, R. Wunder, and V. G. Riggs, IEEE Electron Device Lett. EDL-6 (1985) 384

III,A.4: A. Katsui and S. Tohno, J. Crystal Growth 79 (1986) 287

III,A.5: H. Kanber and D. C. Wang, IEEE Electron Device Lett. EDL-8 (1987) 263

III,A.6: H. Miyari, T. Inada, M. Eguchi, and T. Fukuda, J. Crystal Growth 79 (1986) 291

III,A.7: W. A. Gault, E. M. Monberg, and J. E. Clemans, J. Cryst. Growth 74 (1986) 491

III,A.8: C. L. Reynolds, W. C. Gibson, and J. E. Clemans, Electron. Lett. 23 (1987) 1222

III,A.9: T. Inada, T. Fujii, M. Eguchi, and T. Fukuda, Appl. Phys. Lett. 50 (1987) 86

III,A.10: R. Fischer, D. Neuman, H. Zabel, H. Morkoc, C. Choi, and N. Otsuka, Appl. Phys. Lett. 48 (1986) 1223

III,A.11: J. Varrio, H. Asonen, A. Salokatve, M. Pessa, E. Rauhala, and J. Keinonen, Appl. Phys. Lett. 51 (1987) 1801

III,A.12: T. Soga, T. Imori, M. Umeno, and S. Hattori, Japan. J. Appl. Phys. 26 (1987) L536

III,A.13: III-V Technology Review, Vol. II, No. 3 (1987) 11

III,A.14: G. W. Turner, H. K. Choi, and B.-Y. Tsaur, IEEE Electron Device Lett. EDL-8 (1987) 460

III,A.15: M. Eron, G. Taylor, R. Menna, S. Y. Narayan, and J. Klatskin, IEEE Electron Device Lett. EDL-8 (1987) 350

III,A.16: M. Razeghi, J. Ramdani, H. Verriele, D. Decoster, M. Constant, and J. Vanbremeersch, Appl. Phys. Lett. 49 (1986) 215

III,A.17: A. G. Dentai, J. C. Campbell, C. H. Joyner, and G. J. Qua, Electron. Lett. 23 (1987) 38

III,A.18: P. D. Hodson, R. H. Wallis, and J. I. Davies, Electron. Lett. 23 (1987) 273

III,A.19: A. Suzuki, T. Itoh, T. Terakado, K. Kasahara, K. Asano, Y. Inomoto, H. Ishihara, T. Torikai, and S. Fujita, Electron. Lett. 23 (1987) 954

III,A.20: K. Asano, K. Kasahara, and T. Itoh, IEEE Electron Device Lett. EDL-8 (1987) 289

III,A.21: A. Seki, F. Konushi, J. Kudo, S. Kakimoto, T. Fukushima, and M. Koba, Japan. J. Appl. Phys. 26 (1987) L1587

III,A.22: M. K. Lee, D. S. Wuu, and H. H. Tung, Appl. Phys. Lett. 50 (1987) 1725

III,A.23: S. Shimizu and S. Komiya, J. Cryst. Growth 81 (1987) 243

III,A.24: P. D. Hodson, R. R. Bradley, J. R. Riffat, T. B. Joyce, and R. H. Wallis, Electron. Lett. 23 (1987) 1094

III,A.25: K. Oe and H. Takeuchi, Japan. J. Appl. Phys. 26 (1987) L120

III.B. **Epitaxy**

Figure 1 shows the lattice constants and bandgaps of some III-V compounds and ternary alloys. Aluminum arsenide (AlAs) has a lattice constant very close to that of GaAs which allows the formation of excellent heterojunctions between GaAs and $Al_xGa_{1-x}As$ with the composition index x determining the bandgap of the ternary alloy. Prominent ternary alloys lattice matched to InP are $In_{0.53}Ga_{0.47}As$ and $In_{0.52}Al_{0.48}As$. A variety of ternary and quaternary alloys can actually or potentially be deposited lattice matched to GaAs or InP substrates. For instance, $AlAs_xSb_{1-x}$ might be used as a barrier material on InP, either for a modulation doped field effect transistor (MODFET), or undoped as the insulator in a heterojunction insulated gate field effect transistor (HIGFET), but many of these materials are poorly understood and difficult to grow. $GaAs_{0.51}Sb_{0.49}$, lattice matched to InP, with a bandgap corresponding to about 1.6 μm, of interest for optoelectronics, has recently been investigated (III,B.1).

The number of possible combinations has increased with the realization of strained-layer structures, i.e., the heteroepitaxy of materials which, by themselves, have different lattice constants, but in sufficiently thin layers of the order of nm can form excellent pseudomorphic heterojunctions; the longtime stability of such structures has yet to be sufficiently explored. For thicker layers, the stress due to lattice mismatch is relaxed by MISFIT dislocations which are detrimental to material characteristics.

In growth methods, emphasis is shifting from the mature approaches of liquid phase epitaxy (LPE) and chloride or hydride vapor phase epitaxy (VPE) to metal-organic chemical vapor deposition (MOCVD) and molecular beam epitaxy (MBE) which are preferable for multilayer heterojunction and quantum-well growth

and for compounds and alloys containing aluminum. The growth of phosphorus containing materials such as InP presents a problem for conventional MBE because the high vapor pressure and hygroscopic properties of phosphorus tend to contaminate ultra high vacuum (UHV) systems (III,B.2). MBE has the advantage of exact control of doping and compositional profiles, the disadvantage of high complexity, and expense and of low wafer throughput. MOCVD, for epitaxial deposition more accurately designated as organometallic vapor phase epitaxy (OMVPE), has the advantage of simple source handling by mass flow controllers, low defect densities, and high growth rates if desired, allowing for large scale production. The source gases used in MOCVD present potential safety hazards: the group III alkyls such as trimethylgallium and trimethylindium are pyrophoric, and the group V hydrides, phosphine and particularly arsine, are highly toxic. Attempts to replace these hydrides by less hazardous compounds are in progress. A recent comparison of MOCVD with other epitaxial growth methods is presented in reference III,B.3.

Hybrid approaches have been developed starting either from MOCVD or from MBE. MOCVD can be performed either at atmospheric pressure or at low pressure, down to the Torr range. For pressures above 10^{-2} Torr, the gas flow is viscous; the chemicals diffuse through a a stagnant carrier gas boundary layer above the heated substrate, dissociate, and are deposited (III,B.4). At pressures below 10^{-4} Torr, the mechanism changes to molecular beam transport, resulting in metal-organic molecular beam epitaxy (MOMBE). Starting from MBE, the conventional approach uses condensed effusion sources; this has disadvantages, particularly for the group V elements, which may be overcome by the use of gas sources such as arsine and phosphine (III,B.5), leading to gas source molecular beam epitaxy (GSMBE) (III,B.6). The opposite approach, combining a solid group V (As) source in MBE with a metal alkyl (trimethylgallium) source, is also being pursued (III,B.7). Using both hydrides and metal alkyls in MBE results again in MOMBE which combines the advantages of conventional MBE with easy flux control of MOCVD (III,B.8) but shares with MBE the disadvantages of the complexity and high cost of a UHV technique. Similar hybrid approaches are chemical beam epitaxy (CBE) developed at AT&T Bell Laboratories (III,B.4), and vacuum chemical epitaxy (VCE) developed at Chevron Research Company (III,B.9).

A technique called molecular/ion beam epitaxy (MIBE) (III,A.23), applied to the epitaxy of lattice mismatched materials such as InP on Si substrates, combines an In molecular beam with a mass separated low energy (100 eV) P^+ ion beam to form strain free InP with an intermediate compositionally graded layer in the interface region due to atomic mixing induced by the ion irradiation.

Migration-enhanced epitaxy (MEE) (III,B.10) is an MBE related approach which permits low temperature (below 300°C) growth of GaAs and AlAs by offering the group III and group V elements alternately, allowing deposited Ga or Al atoms to migrate rapidly to appropriate lattice positions. This kind of deposition, which results in the formation of approximately one molecular layer per cycle, has been applied to the growth of GaAs on Si (III,A.11). A related approach, offering the group III and group V elements alternately in GSMBE or MOCVD and growing one molecular layer per cycle in a self-regulated fashion, is atomic layer epitaxy (ALE). A variety of II-VI and III-V compounds have been grown by this technique (III,B.11), as well as Ga-As-In-As superalloy (II,C.16).

Extremely good modulation-doped heterostructures with active InGaAs layers on InP substrates have been grown by atmospheric pressure MOCVD. Room temperature electron mobilities of 11300 cm^2/Vs with sheet electron densities up to 2×10^{12} cm^{-2} have been measured for the 2-D electron gas in InGaAs/InP structures (III,B.12); even higher values, 11500 cm^2/Vs with 2.7×10^{12} cm^{-2} electrons have been obtained for InGaAs/InAlAs (III,B.13). Good luminescent properties of InGaAs/InP QWs down to a thickness of 6 Å have been obtained at NOSC by low pressure MOCVD.

InAlGaAs has been grown lattice matched on InP by pulsed MBE in the form of an $[In_{0.52}Ga_{0.48}As]_m/[In_{0.52}Al_{0.48}As]_n$ superalloy with m and n indicating the number of monolayers in each period (III,B.14).

Semi-insulating Fe doped InGaAs has been demonstrated at NOSC by LPE (III,B.15). Epitaxial SI Fe-doped InP can be grown by MOCVD or LPE (III,B.16). SI InP has been grown by VPE (II,B.4), but the density of deep traps produced by this approach seems to be too low to provide effective insulation for practical voltage biases.

Efforts to grow Co doped SI InGaAsP by LPE are in progress at University of Southern California (USC).

Recent efforts aim at the doping of Si and III-V semiconductors by RE elements such as ytterbium (Yb) and erbium (Er) for photoemitters (III,B.17). The low solubility restricts RE doping by LPE to densities of the order of 10^{16} cm^{-3}. Higher RE densities can be obtained by growth methods which are not confined to thermal equilibrium: InP MOCVD layers have been grown with an RE density of mid 10^{18} cm^{-3}, and MBE has given Si and GaAs layers with up to 2 x 10^{19} RE atoms per cm^3. MOCVD grown RE-doped InP seems to be of better quality than RE-ion-implanted InP (III,B.18).

III,B.1: J. Klem, D. Huang, H. Morkoc, Y. E. Ihm, and N. Otsuka, Appl. Phys. Lett. 50 (1987) 1364

III,B.2: W. T. Tsang, R. C. Miller, F. Capasso, and W. A. Bonner, Appl. Phys. Lett. 41 (1982) 467

III,B.3: P. Burggraaf, Semiconductor International, Nov 1986, p 46

III,B.4: W. Tsang, J. Cryst. Growth 81 (1987) 261

III,B.5: M. B. Panish, J. Electrochem. Soc. 127 (1980) 2729

III,B.6: M. B. Panish, H. Temkin, and S. Sumski, J. Vac. Sci. Technol. B 3 (1985) 657

III,B.7: H. D. Shih, B. Kim, and M. Wurtele, Electron. Lett 23 (1987) 1141

III,B.8: K. Werner, H. Heinecke, M. Weyers, H. Luth, and P. Balk, J. Cryst. Growth 81 (1987) 281

III,B.9: L. M. Fraas, P. S. McLeod, L. D. Partain, R. E. Weiss, and J. A. Cape, J. Cryst. Growth 77 (1986) 386

III,B.10: Y. Horikoshi, M. Kawashima, and H. Yamaguchi, Japan. J. Appl. Phys. 25 (1986) L868

III,B.11: C. H. L. Goodman and M. V. Pesa, J. Appl. Phys. 60 (1986) R65

III,B.12: L. Aina, M. Mattingly, and B. Potter, Appl. Phys. Lett. 51 (1987) 1735

III,B.13: M. Kamada, H. Ishikawa, M. Ikeda, Y. Mori, and C. Kojima, Electron. Lett. 22 (1986) 1147

III,B.14: T. Fujii, Y. Nakata, Y. Sugiyama, and S. Hiyamizu, Japan. J. Appl. Phys. 25 (1986) L254

III,B.15: A. R. Clawson, D. P. Mullin, and D. I. Elder, J. Cryst. Growth 64 (1983) 90

III,B.16: M. Sugawara, M. Kondo, K. Nakai, A. Yamaguchi, and K. Nakajima, Appl. Phys. Lett. 50 (1987) 1432

III,B.17: H. Ennen, Solid State Device Conference, Tokyo, 1987

III,B.18: K. Uwai, H. Nakagome, and K. Takahei, Appl. Phys. Lett. 50 (1987) 977

III.C. Ion Implantation and Diffusion

While ion implantation into InP has been used with reasonable success, it faces problems with the prescription of implant conditions and, in particular for SI InP, with the Fe compensation.

The Fe density in SI bulk InP increases from the top to the bottom of the boule and is usually not well enough characterized in commercially available wafers. This requires preliminary implantation experiments to determine the proper device implantation doses. Furthermore, the annealing required after ion implantation for implant activation can cause Fe redistribution, even for rapid thermal annealing. Chromium doped GaAs had a similar problem which has been alleviated with the use of undoped SI GaAs.

To obtain the desired implant densities and profiles, implantation conditions are set in accordance with the theory of Lindhard, Scharff, and Schiott (LSS) and its tabulated results. This works well for Si, requires minor corrections for GaAs, but gives major deviations for InP (III,C.1) because of the large mass differences of the In and P atoms.

Proton bombardment converts semiconducting GaAs into semi-insulating material which is probably caused by the creation of deep native defects in GaAs. For InP it seems preferable to use heavier ions such as helium (III,C.2) or oxygen (III,C.3); on p-type InP a resistivity of 10^9 Ohm-cm is obtainable but on n-type InP the maximum resistivity achievable by bombardment is of the order of 10^3 Ohm-cm, probably due to the more shallow native defects in the upper half of the conduction band of InP.

Implantation of RE ions with energies up to 6 MeV into Si and III-V materials for optoelectronic applications is pursued by NRL (III,C.3).

A flexible process to fabricate planar microstructures with submicron resolution is focused ion beam (FIB) implantation (III,C.4) with the ion beam focused to 0.1 μm diameter and scanned across the sample to form doped regions of desired patterns. FIB technology is under development by NOSC.

Diffusion of Zn for p-doping of InP is an important technique for forming p-n junctions and for achieving high surface doping concentrations for ohmic contacts. Diffusion in InP is a complicated and poorly understood process. More than one diffusion front has been observed (III,C.5). Diffusion coefficients and activation energies are different for diffusion into undoped and into S-doped InP (III,C.6).

III,C.1: C. R. Zeisse, R. G. Wilson, and C. G. Hopkins, J. Appl. Phys. 57(1985) 1656

III,C.2: M. W. Focht, A. T. Macrander, B. Schwartz, and L. C. Feldman, J. Appl. Phys. 55 (1984) 3859

III,C.3: H. Dietrich, personal communication

III,C.4: T. Hiramoto, T. Ogadiri, P. Oldiges, T. Saito, and T. Ikoma in Gallium Arsenide and Related Compounds, Las Vegas, 1986, Inst. Phys. Conf. Ser. No. 83, p. 295

III,C.5: H. Jung and P. Marschall, Electron. Lett. 23 (1987) 1010

III,C.6: H. S. Marek and H. B. Serreze, Appl. Phys. Lett. 51 (1987) 2031

III.D. **Insulators**

Of interest as insulators for gate insulation, surface passivation, and semiconductor-on-insulator (SOI) technology are three types of materials: amorphous insulators such as silicon dioxide (SiO_2), wide band semiconductors acting as quasi-insulators, and organic insulators such as polyimide.

The high insulator quality of thermal SiO_2 and its compatibility with Si is probably the main reason for the dominant role of Si in semiconductor electronics. Silicon metal-oxide-semiconductor (MOS) technology is based on the insulation of FET gates by SiO_2. Recent investigations (III,D.1) suggest that the excellent properties of technical Si/SiO_2 structures are due to the presence of two to three monolayers of crystalline SiO_2 between the Si and the amorphous SiO_2, with the crystalline SiO_2 lattice matched to the underlying silicon. The lateral extension of the SiO_2 grains forming the intermediate layer can be of the order of millimeters. This crystalline region of SiO_2 appears to occur also in naturally grown SiO_2, but with a grain size of the order of nanometers; the electronic states on the grain boundaries are probably responsible for the observed high density of surface states of naturally grown SiO_2/Si interfaces.

Native oxides of III-V compounds are not practical as insulators, although efforts in this direction continue (III,D.2). Surface passivation of GaAs can be achieved with deposition of Si_3N_4 or SiO_2, with organic layers such as polyimide, or with recently demonstrated spin-coated sulfide films (III,D.3), but gate insulation on GaAs by direct deposition of these insulators does not seem feasible. However, preliminary results on the

pseudomorphic growth of 1.5 nm of Si followed by the deposition of 15 nm of SiO_2 on GaAs shows an unpinned surface Fermi level allowing accumulation, depletion, and inversion of the GaAs surface (III,D.4) which may have a tremendous impact on III-V semiconductor electronics.

For InP and InGaAs, MIS technology exists with insulators such as SiO_2, Si_3N_4, Al_2O_3, and AlP_xO_y. An example of a recent effort is the plasma enhanced chemical vapor deposition (PECVD) of hydrogenated amorphous silicon nitride on InP in the presence of arsine (III,D.5); a similar approach, but without the use of arsine, has been developed by NOSC for the passivation of p-i-n photodiodes. A remaining problem with InP and InGaAs metal-insulator-semiconductor field effect transistors (MISFETs) is that of an electrical instability, or current drift, i.e., a change of the drain current with time for constant drain and gate biases (III,D.6). This drift is probably related to charge trapping in the interface region. A current drift of less than 3% for 10^5 s has been reported (III,D.7), but these measurements were performed under pulsed conditions: measuring current drift as a function of time, the bias was applied while obtaining a measurement point, but turned off between measurements.

In comparison, good semiconductor-semiconductor junctions do not suffer from Fermi level pinning or current drift. Structures such as CaF_2 on InP, CdTe on GaAs, and MnSe or ZnSe on GaAs are under investigation to probe the utility of deposited wide bandgap semiconductors to act as insulators. To obtain pseudomorphic growth of these wide bandgap semiconductors, the layer thickness has to be kept of the order of a few nm or less. If thicker layers are required and the good junction properties are to be retained, either the wide bandgap compounds can be replaced by lattice matched alloys, such as $Ca_xSr_{1-x}F_2$, or a superlattice of alternate thin layers, such as MnSe/ZnSe, of appropriate thickness ratios can be formed. Existing differences in the thermal expansion coefficients of semiconductor and insulator cause mechanical strain which can be alleviated by low temperature deposition and rapid thermal annealing (III,D.8). A brief survey of various halide and oxide insulators has been given by Schowalter et al (III,D.9).

To demonstrate the potential of wide bandgap semiconductors to act as the insulator in SOI technology, GaAs/$Ca_xSr_{1-x}F_2$/GaAs

structures have been grown (III,D.10). Growth of GaAs on SOS has been reported in reference III,A.14.

III,D.1: A. Ourmazd, D. W. Taylor, J. A. Rentschler, and J. Bevk, Phys. Rev. Lett. 59 (1987) 213

III,D.2: K. N. Bhat and N. Basu, Electron. Lett. 23 (1987) 1329

III,D.3: B. J. Skromme, C. J. Sandroff, E. Yablonovitch, and T. Gmitter, Appl. Phys. Lett. 51 (1987) 2022

III,D.4: M. Yoder, personal communication

III,D.5: B. Commere, M. C. Habrard, S. K. Krawczyk, and J. C. Bruyere, Appl. Phys. Lett. 51 (1987) 2142

III,D.6: C. R. Zeisse, M. J. Taylor, and J. C. Boisvert, Proc. Symp. "Dielectric Films on Compound Semiconductors," edited by V. J. Kapoor, D. J. Connolly, and Y. H. Wong, publ. by Electrochemical Society, Vol. 86-3 (1986) 180

III,D.7: K. P. Pande, M. A. Fathimulla, D. Gutierrez, and L. Messick, IEEE Electron Dev. Lett. EDL-7 (1986) 407

III,D.8: R. Singh, F. Radpour, J. Jarayan, S. P. Joshi, M. Rahmati, S. A. Anandkuyan, and S. K. Kahng, Proc. Materials Research Soc., Fall 1986 Symposia C (in press)

III,D.9: L. J. Schowalter and R. W. Fathauer, J. Vac. Sci. Technol. A 4 (1986) 1026

III,D.10: K. Tsutsui, T. Nakazawa, T. Asano, H. Ishiwara, and S. Furukawa, IEEE Electron Device Lett. EDL-8 (1987) 277

III.E. **Metal Contacts**

The basic metal-semiconductor contacts under consideration are Schottky barriers and ohmic contacts. To have sufficiently low leakage currents, Schottky barriers have to be at least 0.6 to 0.8 eV high for most room temperature applications. Ohmic contacts require either a sufficiently low barrier (preferably no

barrier at all), or a barrier which is sufficiently thin that electrons can easily tunnel through, or combinations thereof.

In GaAs the native surface donor near midgap gives a Schottky barrier of about 0.8 eV on n-type material, rather independent of the metal and the processing methods. For ohmic contacts, the conventional approach in GaAs is to make the barrier thin by high doping of the semiconducting surface region, either by alloying an Au-Ge-Ni contact, the common scheme for n-GaAs, or by heavy doping of the surface region before metallization which avoids alloying. Barrier formation can be prevented by the use of compositionally graded epitaxial layers such as n-GaAs/n^+-$Ga_{1-x}In_xAs$/n-InAs under the metal. Nonalloyed contacts have the advantage of improved surface morphology, uniformity and reduced orientation effects. For AlGaAs/GaAs MODFETs, nonalloyed contacts with specific resistances of 4.8×10^{-7} Ohm-cm^2 have recently been achieved by use of an n^+-InGaAs cap layer (III,E.1).

Schottky barriers on InP remain poorly understood. On n-InP, barrier heights of 0.33 eV for Ni, Al, Sn, and Mn, of 0.43 eV for Pd, Cu, Au, and Cr, and of 0.54 eV for Ag have been found (III,E.2). Larger Schottky barriers of 0.6 - 0.7 eV for electroplated Cd, and about 0.9 eV for Hg were recently reported by UCSD/NOSC (III,E.3). A Langmuir-Blodgett technique for the deposition of Cd gates, avoiding problems with electroplating or evaporation, has been demonstrated on InGaAs (III,E.4).

Ohmic Au-Ge contacts with contact resistances of less than 10^{-5} Ohm-cm^2 are readily achieved on n-type InP and InGaAs. Ohmic contacts on p-type material are more difficult to fabricate and are under development as are ohmic contacts using refractory metals.

III,E.1: S. Kuroda, N. Harada, T. Katakami, and T. Mimura, IEEE Electron Device Lett. EDL-8 (1987) 389

III,E.2: N. Newman, T. Kendelewicz, L. Bowman, and W. E. Spicer, Appl. Phys. Lett. 46 (1985) 1176

III,E.3: L. G. Meiners, A. R. Clawson, and R. Nguyen, Appl. Phys. Lett. 49 (1986) 340

III,E.4: W. K. Chan, H. M. Cox, J. H. Abeles, and S. P. Kelty, Electron. Lett. 23 (1987) 1346

III.F. Etching and Cleaving

To fabricate wells in InP with vertical walls and a smooth bottom surface for the regrowth of InP surface-oriented Gunn diodes on SI InP substrates, a variety of wet etch approaches have been examined at NOSC (III,F.1).

Leakage currents of mesa structures are frequently dominated by conduction along the mesa walls and can be drastically reduced by using appropriate wet etches as demonstrated for InGaAs/InP double-barrier resonant tunneling diodes (III,F.2).

A variety of plasma etching techniques (III,F.3) are available or under development for III-V compounds and alloys. Chemically assisted ion beam etching (CAIBE) has shown to give a high yield of AlGaAs/GaAs ridge waveguide lasers on MOCVD wafers (III,F.4).

Facets for discrete injection laser diodes are made by cleaving. For IOECs this is usually not feasible and the alternatives are facet etching which increases the threshold current and decreases efficiency, or microcleavage (III,F.5) which gives high performance LDs, but the reproducibility and yield of which has yet to be determined.

III,F.1: M. J. Taylor and E. R. Schumacher, NOSC TN-1521, Feb 1988

III,F.2: T. H. H. Vuong, D. C. Tsui, and W. T. Tsang, Appl. Phys. Lett. 50 (1987) 1004

III,F.3: L. Henry, C. Vaudry, and P. Granjoux, Electron. Lett. 23 (1987) 1253

III,F.4: L. D. Zhu, G. A. B. Feak, R. J. Davis, and J. M. Ballantyne, IEEE J. Quantum Electronics QE-23 (1987) 309

III,F.5: H. Nobuhara, O. Wada, and T. Fujii, Electron. Lett. 21 (1985) 718

IV. DEVICES, INTEGRATED CIRCUITS AND APPLICATIONS

IV.A. Millimeter Wave Diodes

Transferred electron devices (TEDs), also designated as Gunn devices, are of interest for mm-wave low noise oscillators and amplifiers. Above 40 GHz, InP mm-wave Gunn diodes (IV,A.1) are clearly superior over their GaAs counterparts. While GaAs Gunn diodes are expected to work to about 100 GHz, InP Gunn diodes have been demonstrated up to 140 GHz (IV,A.2) and, according to the shorter energy relaxation time of InP, should operate up to 200 GHz. The higher peak-to-valley velocity ratio of InP gives higher efficiency of InP Gunn devices and the higher threshold field and lower hot electron diffusion coefficient leads to lower noise. A medium power (50 mW) wide band (75 to 110 GHz) InP Gunn amplifier has been developed in a joint Varian/NOSC effort (IV,A.3). Oscillations on surface-oriented Gunn diodes on SI InP for monolithic integration have been observed at NOSC.

Transferred electron effects in InGaAs and InGaAsP have been investigated and pulsed InGaAs TEDs have been demonstrated (IV,A.4); InGaAs may promise high efficiency Gunn diodes because of the high peak velocity, large NDR and low threshold field, but the small difference between the bandgap energy and the Gamma-L energy separation leads to avalanche breakdown for voltages not much beyond threshold.

InP impact ionization avalanche transit time (IMPATT) diodes (IV,A.5) are expected to show higher efficiency in the 30 to 100 GHz range and lower noise compared to Si and GaAs, but lack of recent activity in this area seems to indicate that theoretical expectations may not have been met.

Quantum-well injection transit-time (QWITT) devices, using a double-barrier resonant-tunneling (DBRT) structure for carrier injection, with performance superior to TEDs or IMPATTs, have been proposed (IV,A.6), (IV,A.7).

DBRT diodes (also abbreviated as DBDs, resonant tunneling barrier (RTB) structures, resonant tunneling (RT) diodes, etc.) may

exhibit NDR. AlGaAs/GaAs DBRT diodes have had the longest development; peak-to-valley current ratios of 3.9 at room temperature have been achieved (IV,A.8). Improved performance has been obtained for AlAs barriers: oscillations up to 56 GHz (IV,A.9) and, more recently, at 104 to 108 GHz (IV,A.10) have been observed. Oscillation frequencies up to several 100 GHz or even into the low THz region (IV,A.11) have been predicted by theory. For logic applications, switching times of 100 fs have been calculated (IV,A.12). By monolithic integration of two DBRT diodes, a device with two peaks in the I-V characteristics has been demonstrated (IV,A.13) which can serve as three-state memory cell for multiple-valued logic and other applications.

In other material systems, RF operation of DBRT diodes has yet to be demonstrated. The highest peak-to-valley current ratios of 14 at room temperature and 35 at 77°K have been achieved for pseudomorphic AlAs/InGaAs DBRT diodes on InP (IV,A.14). For lattice matched InAlAs/InGaAs on InP, current ratios of 4 at room temperature and 15 at 80°K have been obtained (IV,A.15). The development of InGaAs/InP is less advanced; diodes with current ratios of 1.9 at 77°K and 3.1 at 4.2°K have been obtained by CBE (III,F.2).

For the above DBRT diodes, the same material is used in the well and as outer contacts to the barriers. More design flexibility is available for a demonstrated strained-layer $In_{0.2}Ga_{0.8}As$ QW with $Al_{0.25}Ga_{0.75}As$ barriers and GaAs contacts, all on GaAs substrates, where the QW has a negative conduction band offset with respect to the GaAs contacts (IV,A.16). Below 100°K a peak-to-valley current ratio of 2.6 has been observed which degrades rapidly above this temperature.

IV,A.1: L. Wandinger, Microwave Journal, March 1981, p. 71

IV,A.2: I. G. Eddison, I. Davies, and D. M. Brookbanks, MSN February 1982, p. 91

IV,A.3: P. H. Wolfart and D. Rubin, NOSC TD 1077, April 1987

IV,A.4: W. Kowalsky and A. Schlachetzki, Solid-State Electron. 28 (1985) 299

IV,A,5: F. B. Fank, J. D. Crowley, and J. J. Berenz, Microwave Journal, June 1979, p. 86

IV,A.6: V. P. Kesan, D. P. Neikirk, B. G. Streetman, and P. A. Blakey, IEEE Electron Device Lett. EDL-8 (1987) 129

IV,A.7: I. Song and D.-S. Pan, IEEE Electron Device Lett. EDL-8 (1987) 560

IV,A.8: C. I. Huang, M. J. Paulus, C. A. Bozada, S. C. Dudley, K. R. Evans, C. E. Stutz, R. L. Jones, and M. E. Cheney, Appl. Phys. Lett. 51 (1987) 121

IV,A.9: T. C. L. G. Sollner, E. R. Brown, W. D. Goodhue, and H. Q. Le, Appl. Phys. Lett. 50 (1987) 332

IV,A.10: T. C. L. G. Sollner, E. R. Brown, and W. D. Goodhue, Picosecond Electronics and Optoelectronics, 1987 Technical Digest Series, Optical Society of America, Vol. 1, p. 143

IV,A.11: W. R. Frensley, Third International Conference on Superlattices, Microstructures & Microdevices, Chicago, IL, 17-20 August 1987

IV,A.12: H. C. Liu and D. D. Coon, Appl. Phys. Lett. 50 (1987) 1246

IV,A.13: F. Capasso, S. Sen, A. Y. Cho, and D. Sivco, IEEE Electron Device Lett. EDL-8 (1987) 297

IV,A.14: T. Inata, S. Muto, Y. Nakata, S. Sasa, T. Fujii, and S. Hiyamizu, Japan. J. Appl. Phys. 26 (1987) L1332

IV,A.15: S. Sen, F. Capasso, A. L. Hutchinson, and A. Y. Cho, Electron. Lett. 23 (1987) 1229

IV,A.16: M. A. Reed and J. W. Lee, Appl. Phys. Lett. 50 (1987) 845

IV.B. Transistors and Integrated Circuits

The critical dimension determining speed of a transistor is that along the current flow. Conventional FET structures are of the lateral type with the current flowing parallel to the surface and the critical length dimension limited by lithographic capabilities. For vertical structures such as the vertical FET (VFET), permeable base transistor (PBT), heterojunction bipolar transistor (HBT), and hot electron transistor (HET), the current flow is perpendicular to the surface and the critical dimension is the layer thickness which allows much better control than can be a achieved by lithography. Vertical devices are more compact than lateral structures, do not suffer from current leakage through the substrate, and are the elements for vertical integration which allows implementation of new functions. Fabrication of the VFET and PBT is technologically demanding and has been demonstrated for GaAs, but not for InP where the low Schottky barrier may represent a problem similarly as for conventional MESFETs. A brief review of mm-wave transistors including VFETs and PBTs has recently been given by Murphy and Zeidler (IV,B.1).

Incorporation of resonant tunneling double barrier structures in various transistor structures has been proposed or realized (IV,B.2), (IV,B.3). High frequency operation should be possible, but has yet to be demonstrated.

FET electronics in direct bandgap semiconductors such as GaAs, InP and InGaAs emphasizes n-channel technology because of the large electron-to-hole mobility ratios, although complementary GaAs technology utilizing n- and p-channels is being explored (IV,B.4). Depletion (D) type FETs are normally on, enhancement (E) type FETs are normally off. For the FETs under consideration, with exception of E-MISFETs and E-HIGFET, the electrons in the n-channel are provided by n doping, either by doping the channel directly, or by doping an adjacent wider bandgap semiconductor from where electrons spill into the channel (modulation or selective doping).

IV,B.1: J. D. Murphy and J. R. Zeidler, IEEE GaAs IC Symposium (1987), p. 33

IV,B.2: T. K. Woodward, T. C. McGill, H. F. Chung, and R. D. Burnham, Appl. Phys. Lett. 51 (1987) 1542

IV,B.3: W. Lee and C. G. Fonstad, IEEE Electron Device Lett. EDL-7 (1986) 683

IV,B.4: S. M. Baier, G.-Y. Lee, H. K. Chung, B. J. Fure, and R. Mactaggart, IEEE Electron Device Lett. EDL-8 (1987) 260

IV.B.1. Metal-Semiconductor FETs (MESFETs)

GaAs FET electronics is dominated by MESFET technology made possible by the relatively large Schottky barrier of about 0.8 eV. To turn off a depletion (D) type MESFET requires application of a reverse bias to the gate, restricted only by the Schottky barrier breakdown voltage which is of the order of 10 V for a carrier density of 10^{17} and higher for smaller densities; this allows for a large voltage margin, puts little demands on manufacturing tolerances, and makes the depletion MESFET (D-MESFET the preferred choice in GaAs whenever possible. In contrast, turning on an enhancement MESFET (E-MESFET) with a given forward bias while keeping the gate current small is a much more delicate task requiring stringent control of material parameters and manufacturing processes to restrict threshold voltage variations to 0.05 V or less. Gate lengths of 0.5 or 0.25 μm are state of the art in GaAs technology, and 0.1 μm gates have been demonstrated (IV,B1.1), (IV,B1.2). Recent GaAs power MESFETs with gate length of 0.25 μm (IV,B1.3) and 0.35 μm (III,B.7), respectively, gave about 0.6 W/mm power density at approximately 30% power added efficiency (PAE). In spite of the commercial maturity of GaAs MESFETs, properties such as backgating and low frequency oscillations are poorly understood (IV,B1.4). Status and problems of GaAs microelectronics are further discussed in reference IV,B1.5.

The first GaAs MESFETs grown by MBE on SI InP substrate with a 0.5 μm GaAs buffer layer for monolithic integration with InP based photonic devices have shown good performance characteristics (III,A.20).

InP MESFETs have been demonstrated (IV,B1.6), but the low Schottky barriers of 0.3 - 0.5 eV make InP MESFET technology impractical. Incorporation of a native oxide between metal and semiconductor can raise the barrier height as high as 0.85 eV, but these results seem somewhat irreproducible. InP D-MESFETs with Cd gates of barrier heights of of 0.6 - 0.7 eV have been demonstrated (III,E3) in a joint effort by UCSD and NOSC.

IV,B1.1: H. Jaeckel, V. Graf, B. J. van Zeghbroeck, P. Vettiger, and P. Wolf, IEEE Electron Device Lett. EDL-7 (1986) 522

IV,B1.2: G. A. Sai-Halasz, M. R. Wordeman, D. P. Kern, E. Ganin, S. Rishton, D. S. Zicherman, H. Schmid, M. R. Polcari, H. Y. Ng, P. J. Restle, T. H. P. Chang, and R. H. Dennard, IEEE Electron Device Lett. EDL-8 (1987) 463

IV,B1.3: B. Kim, M. Wurtele, H. D. Shih, and H. Q. Tserng, Electron. Lett. 23 (1987) 1008

IV,B1.4: J. F. Wager and A. J. McCamant, IEEE Trans. Electron Devices ED-34 (1987) 1001

IV,B1.5: III-V Microelectronics Panel Report, Science Applications International Corporation, ET-TAR-1001, SInP power depletion 29 July 1987

IV,B1.6: J. S. Barrera and R. J. Archer, IEEE Trans. Electron Devices ED-22 (1975) 1023

IV.B.2. Metal-Insulator-Semiconductor FETs (MISFETs)

Depletion and enhancement type MISFETs with amorphous insulators such as SiO_2 have been developed for InP (IV,B2.1) and InGaAs (IV,B2.2) during the last 10 years by NOSC and others. Power gain on GaAs MISFETs with anodic oxides has been shown at microwave frequencies (IV,B2.3) where the surface states cannot follow the impressed microwave signal, but the high surface state densities prevent low frequency or DC control for GaAs. InP or InGaAs E-MISFETs do not need any n-type doping of the channel; they can be either of the inversion type, made on p-type material, or of the accumulation type, on SI material. The

complications discussed for E-MESFETs do not apply to MISFETs: biases of either sign, short of the insulator breakdown voltage, may be applied to the gate. Radiation effects in the gate oxides of present InP MISFETs are similar to those in non-hardened Si MOSFETs.

A vertical InP E-MISFET on low defect n-InP substrate with a 2 μm thick Fe-doped SI InP layer grown by MOCVD for substrate insulation, borosilicate gate insulator, and V-shaped gate, in structure similar to Si VMOS, has shown a transconductance of 100 mS/mm (IV,B2.4).

The availability of both normally-on (depletion type) and normally-off (enhancement type) MISFETs in InP and InGaAs allows the implementation of direct coupled FET logic (DCFL) with active loads for logic circuits, similar to Si n-channel metal-oxide-semiconductor (NMOS) and GaAs E/D technology. Buffered-output 21-stage planar InP DCFL ring oscillator circuits by NOSC (IV,B2.5) using E-MISFET drivers with source drain separations of 1.5 μm and gate metallization length of 3.0 μm gave a minimum observed propagation delay per stage of 22 ps and a minimum observed power delay product of 84 fJ. These performance data correspond to those of submicron GaAs MESFET logic. More recently, three-input AND/NOR logic gates with 500-700 ps propagation delay per gate, clocked at 1 GHz, have been demonstrated (III,D.7). For an InP inverter with 1 μm gate length E-MISFETs, FET transconductances of 200 mS/mm (IV,B2.6), and more recently of 320 mS/mm (IV,B2.7) have been reported; propagation delays of 25 ps per stage have been observed and digital ICs based on these MISFETs are capable of operating at 5 GHz. The DC drift of InP MISFETs does not present a problem for these and other digital applications because of the large noise margins available.

Medium scale integration of InP MISFETs has been demonstrated on 3 x 3 multipliers (IV,B2.8) and 64-bit static random access memories (SRAMs) (IV,B2.9). The packing density of circuit integration is probably limited by side gating. According to Hasegawa et al (II,B.8), the larger surface breakdown fields in SI InP compared to SI GaAs prevent sidegating which may be a crucial argument in favor of InP large scale integration and beyond.

For high frequency power applications, InP MISFETs, compared to GaAs MESFETs, have the advantage of higher peak velocity, threshold field, and breakdown voltage for the electrons, higher thermal conductivity of the InP, higher applicable gate voltages, and negligible gate leakage currents. Also, the n-channel can be driven into accumulation. NOSC has reported both ion-implanted and epitaxial InP power depletion MISFETs (D-MISFETs) with 1.4 μm gate length and 0.8 to 1.0 mm gate width (IV,B2.10). At 9.7 GHz and 4 dB gain, a power density of 4.5 W/mm with 46% PAE has been achieved for the epitaxial FET, and 2.9 W/mm with 31% PAE for the ion-implanted FET. The power density for the epitaxial FET is higher by a factor of 3 than that for the best reported GaAs or InGaAs FETs. The applied RF gate bias seems to alleviate current drift even in the presence of a superimposed DC bias; an initial power output of 1.5 W was stable to within 2% over 167 hours of continuous operation.

An InP power MISFET by Radio Corporation of American (RCA) (IV,B2.11) with 1 μm gate length has been evaluated at 4, 12, and 20 GHz. At 4 GHz and 8.5 dB gain it gave a power density of 1.13 W/mm with 45% PAE. At 20 GHz with 3.0 dB gain the power density was 0.73 W/mm with 13.6% PAE.

Recently a 0.6 μm gate length InP MISFET has been demonstrated by Nippon Electric Company (NEC) (IV,B2.12) with a power gain cutoff frequency of 64 GHz, a power gain of 6.5 dB in the 30 GHz band, and an output power density of 0.24 W/mm at 1 dB gain compression. This is the first reported submicron InP power MISFET and we expect that higher power densities should be achievable at 30 GHz with improvements in design and technology.

The first InGaAs MISFET digital IC, a ring oscillator on SI InP with 1.2 μm gate length E-MISFET drivers, gave propagation delay times of 50 ps per gate at 9 mW power dissipation per gate (IV,B2.13). More recently, for an InGaAs E-MISFET in an inverter circuit on InP, a propagation delay of 15 ps has been measured by a noninvasive electro-optic technique (IV,B2.14). For an InGaAs power MISFET with 1 μm gate length, performance data have been reported between 4 and 32.5 GHz (IV,B2.15): from S-parameter measurements, f(max) = 45 GHz; at 4 GHz and about 12 dB gain, a power density of 1.53 W/mm with 53% PAE, and 0.78 W/mm with 64% PAE were achieved; for 20 GHz, 0.74 W/mm were obtained with 26% PAE at 3.0 dB gain, and 0.43 W/mm with 32% PAE at 5.7 dB gain.

IV,B2.1: H. H. Wieder, J. Vac. Sci. Technol. 17 (1980) 1009

IV,B2.2: H. H. Wieder, J. L. Veteran, A. R. Clawson, and D. P. Mullin, Appl. Phys. Lett. 43 (1983) 287

IV,B2.3: D. L. Lile, D. A. Collins, L. Messick, and A. R. Clawson, Appl. Phys. Lett. 32 (1978) 247

IV,B2.4: C.-L. Cheng, Y. Ota, B. Tell, J. L. Zilko, S. R. Forrest, and J. W. Fleming, IEEE Electron Device Lett. EDL-7 (1986) 549

IV,B2.5: L. J. Messick, IEEE Transact. Electron Dev. ED-31 (1984) 763

IV,B2.6: A. Antreasyan, P. A. Garbinski, V. D. Mattera, N. J. Shah, and H. Temkin, Electron. Lett. 22 (1986) 1014

IV,B2.7: A. Antreasyan, P. A. Garbinski, V. D. Mattera, and H. Temkin, Picosecond Electronics and Optoelectronics, 1987 Technical Digest Series, Optical Society of America, Vol. 1, p. 19

IV,B2.8: D. K. Kinell, Lockheed Missiles & Space Co., Inc., LMSC F007736, Oct 1984

IV,B2.9: M. D. Clark, R. A. Jullens, and M. Waldner, NOSC TD 1009 Nov 1986

IV,B2.10: L. Messick, D. A. Collins, R. Nguyen, A. R. Clawson, and G. E. McWilliams, Proc. Symposium on Dielectric Films on Semiconductors, Electrochemical Society (1987)

IV,B2.11: P. D. Gardner, S. G. Liu, T. Bibby, S. D. Colvin, and S. Y. Narayan, RADC-TR-87-159 Final Technical Report, Oct 1987

IV,B2.12: NEC Corporation Public Relations Office, JETRO, Nov 1987, p. 9

IV,B2.13: L. C. Upadhyayula, P. D. Gardner, S. G. Liu, and S. Y. Narayan, IEEE Electron Device Lett. EDL-7 (1986) 390

IV,B2.14: J. M. Wiesenfeld, R. S. Tucker, A. Antreasyan, C. A. Burrus, A. J. Taylor, V. D. Mattera, and P. A. Garbinski, Appl. Phys. Lett. 50 (1987) 1310

IV,B2.15: P. D. Gardner, D. Bechtle, S. Y. Narayan, S. D. Colvin, and J. Paczkowski, IEEE Electron Device Lett. EDL-8 (1987) 443

IV.B.3. Junction FETs (JFETs)

In JFETs the n-channel is controlled by the p-n junction while the interface region of the strongly doped p-region with the gate metal plays no active role but merely serves as contact. JFETs can have lower gate leakage currents than MESFETs because the p-n homojunction is higher than the Schottky barrier. This makes InP JFETs a feasible technology as shown by NRL (IV,B3.1). JFETs, compared to MISFETs, have the advantage to be free of drift, but the disadvantage of a non-vanishing gate leakage current. Fully ion-implanted (IV,B3.2), (IV,B3.3) and Zn diffused (IV,B3.4) InP JFETs have been demonstrated with gate lengths of 5, 2, and 1 μm, maximum transconductances of 40, 50, and 35 mS/mm, and f(T) of 2, 6.6, and 7 GHz, respectively, with gate leakage currents at pinch-off well below 20 nA. MOCVD grown epitaxial JFETs are under development at NOSC.

A different design which may avoid channel-substrate interface effects is the p-column JFET which has a periodic array of p^+ columns implanted through the n-channel region; the current flow is modulated by the depletion regions extending laterally from the p-columns. For an InP p-column JFET with a nominal gate length of 1.7 μm, f(T) = 4.5 GHz and f(max) = 16 Ghz were obtained (IV,B3.5).

Radiation hard GaAs MESFET and JFET digital circuits (IV,B3.6) are under development by DARPA for space applications. InP JFETs show radiation hardness superior to that of GaAs MESFETs (II,B.10), but no work on InP JFET ICs seems to have been reported. The combination of higher peak velocity, potentially superior radiation hardness, and less sidegating compared to GaAs suggest InP JFET IC technology as a topic worthwhile of investigation.

InGaAs JFETs with 1.6 μm long gates on SI InP substrates with InP buffer layers have shown a transconductance of 130 mS/mm and f(T) = 20 GHz as obtained from S-parameter measurements (IV,B3.7). More recently, 1 μm gate length InGaAs enhancement junction field effect transistor E-JFETs with transconductances as high as 553 mS/mm have been reported (IV,B3.8).

For n-InGaAs/p-InP heterojunction FETs with 0.5 μm gate length, a transconductance of 260 mS/mm has been obtained (IV,B3.9).

IV,B3.1: J. B. Boos, S. C. Binari, G. Kelner, P. E. Thompson, T. H. Weng, N. A. Papanicolaou, and R. L. Henry, IEEE Electron Device Lett. EDL-5 (1984) 273

IV,B3.2: C.-L. Cheng, K.-W. Wang, and S. M. Parker, IEEE Electron Device Lett. EDL-8 (1987) 483

IV,B3.3: S. J. Kim, K. W. Wang, G. P. Vella-Coleiro, J. W. Lutze, Y. Ota, and G. Guth, IEEE Electron Device Lett. EDL-8 (1987) 518

IV,B3.4: C. Fan and P. K. L. Yu, Electron. Lett. 23 (1987) 981

IV,B3.5: J. D. Woodhouse and J. P. Donnelly, IEEE Electron Device Lett. EDL-7 (1986) 387

IV,B3.6: J. K. Notthoff, R. Zuleeg, and G. L. Troeger, IEEE Trans. Nuclear Sci. NS-30 (1983) 4173

IV,B3.7: J. Selders, H. J. Wachs, and H. Jurgensen, Electron. Lett. 22 (1986) 313

IV,B3.8: H. Albrecht and C. Lauterbach, IEEE Electron Device Lett. EDL-8 (1987) 353

IV,B3.9: J. Y. Raulin, E. Thorngren, M. A. di Forte-Poisson, M. Razeghi, and G. Colomer, Appl. Phys. Lett. 50 (1987) 535

IV.B.4. Heterojunction-Insulated-Gate FETs (HIGFETs)

If the amorphous insulator in a MISFET is replaced by an epitaxially deposited semiconductor which forms a good heterojunction with the underlying semiconductor, this will reduce or eliminate surface states responsible for surface Fermi level pinning, electrical instability, and mobility reduction due to surface scattering. The deposited semiconductor can serve as gate insulator if it has (a) a sufficiently high conduction band offset with respect to the underlying n- channel material, (b) sufficient thickness to prevent tunneling of charge carriers, and (c) sufficiently low carrier density and therefore conductivity, either by itself as for SI material or as a consequence of depletion. Designations such as as heterojunction insulated gate FET (HIGFET), doped-channel MIS-like FET (DMT), or heterostructure MISFET are used for these transistors which can be designed for inversion, depletion, or accumulation mode operation. In the case where the wider bandgap material has no insulating properties by itself, such structures might more appropriately be called buried interface FETs (BIFETs) (IV,B4.1). A related device is the semiconductor-insulator-semiconductor FET (SISFET) (IV,B4.2) which uses a highly doped semiconductor gate layer between the wider bandgap insulating material and the gate metal.

The HIGFET design avoids (a) highly doped active layers under the Schottky gate which reduce the breakdown voltage of MESFETs and MODFETs, and (b) parallel conduction in the higher bandgap semiconductor which reduces the transconductance of MODFETs for high densities of the 2-D electron gas (IV,B4.3).

For an undoped-AlGaAs/n-GaAs HIGFET, a maximum power density of more than 1 W/mm and a maximum power added efficiency of 43% at 19 GHz has been obtained (IV,B4.4). The first high-speed digital undoped-AlGaAs/n-GaAs HIGFET IC has recently been reported (IV,B4.5). For an undoped-AlGaAs/undoped-GaAs HIGFET with 1 μm long tungsten nitride (WN) gate, a room temperature transconductance of 460 mS/mm has been achieved (IV,B4.6).

Depletion mode undoped-InAlAs/n-InP HIGFETs have been demonstrated in a joint effort by UCSD and NOSC (IV,B4.7). The InAlAs composition has been chosen as Al rich rather than lattice matched to InP to increase the conduction band offset.

Following a trend in GaAs MESFETs and HIGFETs to reduce short-channel effects and improve performance by using a thin and heavily doped channel, an undoped-InAlAs/n-InGaAs HIGFET with a Si doped channel of 7 x 10^{17} cm^{-3} has recently been reported to show high performance potential (IV,B4.8).

IV,B4.1: T. J. Drummond, W. Kopp, D. Arnold, R. Fischer, H. Morkoc, L. P. Erickson, and P. W. Palmberg, Electron. Lett. 19 (1983) 986

IV,B4.2: A. T. Yuen, E. L. Hu, S. I. Long, and G. J. Sullivan, IEEE Electron Device Lett. EDL-8 (1987) 272

IV,B4.3: H. Hida, A. Okamoto, H. Toyoshima, and K. Ohata, IEEE Electron Device Lett. EDL-7 (1986) 625

IV,B4.4: B. Kim, H. Q. Tserng, and J. W. Lee, IEEE Electron Device Lett. EDL-7 (1986) 638

IV,B4.5: H. Hida, H. Toyoshima, and Y. Ogawa, IEEE Electron Device Lett. EDL-8 (1987) 557

IV,B4.6: M. Wolny, T. Aguila, P. Deconinck, D. Moroni, and J. P. Andre, Electron Lett. 23 (1987) 1127

IV,B4.7: C. M. Hanson, P. Chu, H. H. Wieder, and A. R. Clawson, IEEE Electron Device Lett. EDL-8 (1987) 53

IV,B4.8: J. A. Del Alamo and T. Mizutani, IEEE Electron Device Lett. EDL-8 (1987) 534

IV.B.5. Modulation Doped FETs (MODFETs)

Modulation doped FETs (MODFETs), also known as high electron mobility transistors (HEMTs), two-dimensional electron gas FETs (TEGFETs) hetero-interface FETs (HIFETs), selectively-doped heterostructure transistors (SDHTs) or multi-acronym device (MAD) (IV,B5.1), have a wider bandgap n-doped semiconductor epitaxially deposited on a narrower bandgap undoped semiconductor resulting in a 2-D electron gas in the interface region of the undoped

material. This combines the advantages of good heterojunction interface properties with the high mobility of the undoped channel.

In the conventional GaAs MODFET, lattice matched n-AlGaAs is deposited on undoped GaAs. Scattering of the electrons in the undoped channel from the electrostatic potentials of the donors in the n-AlGaAs can be reduced by a thin undoped AlGaAs buffer layer. A maximum transconductance of 400 mS/mm has recently been demonstrated for a 0.28 μm gate length AlGaAs/GaAs MODFET (IV,B5.2); with saturated resistor loads, a propagation delay per gate of 9.2 ps with a power dissipation of 4.2 mW per gate has been observed on a 25-stage ring oscillator. For ring oscillators with 0.35 μm gate length MODFETs, a propagation delay of 10.2 ps/gate at 1.03 mW/gate has been reported (IV,B5.3). An 1.1 μm gate length MODFET with nonalloyed ohmic contacts, advantageous for high integration, has exhibited a maximum transconductance of 240 mS/mm (III,E1).

A 0.25 μm gate length AlGaAs/GaAs MODFET gave f(T) = 80 GHz, a noise figure of 2.4 dB at 60 GHz for over 7 dB of associated gain, and a PAE of 42% at 20 GHz (IV,B5.4). For a six-channel power MODFET with 0.5 μm long and 2.4 mm wide gates, an output power of 1 W has been reported at 30 GHz (IV,B5.5).

Transport properties can be improved by using pseudomorphic InGaAs as the channel material. The carrier confinement is better in GaAs/InGaAs/GaAs MODFETs compared to AlGaAs/GaAs. Even better carrier confinement and electron transfer is achieved in AlGaAs/InGaAs/GaAs MODFETs; for 0.25 μm gate length a maximum power added efficiency of 28% and a maximum output power density of 0.4 W/mm has been obtained at 60 GHz; a noise figure of 2.4 dB with associated gain of 4.4 dB has been obtained at 62 GHz (I^{--},B5.6). For a 0.1 μm gate length AlGaAs/InGaAs/GaAs MODFET, a noise figure of 4.2 dB with an associated gain of 6 dB at 60 GHz has been reported (IV,B5.7).

Improvements in the source-drain breakdown voltage and the gate-channel forward turn-on and reverse breakdown voltage by a shallow p-type implantation into the strongly n-doped AlGaAs under the gate have been reported (IV,B5.8). The low-dose p-type implant is insufficient to convert the n-AlGaAs but produces a

region of low net doping, combining some of the advantages of MODFETs and HIGFETs.

The transport properties can be further improved by growing InGaAs layers lattice matched on InP, allowing superior alloy compositions and avoiding strained-layers. InAlAs/InGaAs MODFETs with 1 μm gate length on SI InP have been demonstrated by MBE (IV,B5.9) and by MOCVD (IV,B5.10). An f(max) = 62 GHz, and f(T) = 26.5 GHz were achieved (IV,B5.9); the f(max) is almost twice that obtained for a pseudomorphic AlGaAs/InGaAs MODFET on GaAs of the same geometry. The MOCVD device showed a maximum transconductance as high as 530 mS/mm.

Increasing the InAs mole fraction in InGaAs and the AlAs mole fraction in InAlAs beyond the values for lattice match to InP increases device speed and barrier height, improves carrier confinement, permits a higher carrier sheet density, and reduces the gate leakage current. The occurring strains in the two ternaries are of opposite sign and nearly cancel each other. For an $In_{0.6}Ga_{0.4}As/In_{0.45}Al_{0.55}As$ pseudomorphic E-MODFET with 1.6 μm gate length, a maximum extrinsic transconductance of 271 mS/mm has been reported (IV,B5.11). Eventually, with increasing InAs mole fraction, avalanche breakdown, in the InGaAs, is expected to occur before the peak electron velocity is reached (IV,B5.12).

Inverted InGaAs/InP MODFETs with 1 μm long Cd gates deposited by a Langmuir-Blodgett film technique have been demonstrated with an extrinsic transconductance per gate width of 170 mS/mm and an f(T) of 19 GHz (III,E.4). The inverted structure has the undoped channel layer between the doped InP and the Cd gate. The doped high-bandgap material under the 2-D electron gas can suppress short channel effects, while the small bandgap material on top facilitates formation of ohmic contacts with source and drain.

IV,B5.1: V. Rehn, White Paper "Semiconductor Heterostructure-Device Opportunities and Requisite Research", NWC Code 3813, Oct 1986

IV,B5.2: Y. Awano, M. Kosugi, T. Mimura, and M. Abe, IEEE Electron Device Lett. EDL-8 (1987) 451

IV,B5.3: N. J. Shah, S.-S. Pei, C. W. Tu, and R. C. Tiberio, IEEE Trans. Electron Devices ED-33 (1986) 543

IV,B5.4: J. J. Berenz, Picosecond Electronics and Optoelectronics, 1987 Technical Digest Series, Optical Society of America, Vol. 1, p. 37

IV,B5.5: K. Hikosaka, N. Hidaka, Y. Hirachi, and M. Abe, IEEE Electron Device Lett. EDL-8 (1987) 521

IV,B5.6: T. Henderson, M. I. Aksun, C. K. Peng, H. Morkoc, P. C. Chao, P. M. Smith, K.-H. G. Duh, and L. F. Lester, IEEE Electron Device Lett. EDL-7 (1986) 649

IV,B5.7: P. C. Chao, R. C. Tiberio, K.-H. G. Duh, P. M. Smith, J. M. Ballingall, L. F. Lester, B. R. Lee, A. Jabra, and G. G. Gifford, IEEE Electron Device Lett. EDL-8 (1987) 489

IV,B5.8: C. S. Lam and C. G. Fonstad, IEEE Electron Device Lett. EDL-8 (1987) 563

IV,B5.9: C. K. Peng, M. I. Aksun, A. A. Ketterson, H. Morkoc, and K. R. Gleason, IEEE Electron Device Lett. EDL-8 (1987) 24

IV,B5.10: M. Kamada, T. Kobayashi, H. Ishikawa, Y. Mori, K. Kaneko, and C. Kojima, Electron. Lett. 23 (1987) 297

IV,B5.11: J. M. Kuo, T.-Y. Chang, and B. Lalevic, IEEE Electron Device Lett. EDL-8 (1987) 380

IV,B5.12: S. Krishnamurthy, A. Sher, and A.-B. Chen, J. Appl. Phys. 61 (1987) 1475

IV.B.6. Heterojunction Bipolar Transistors (HBTs)

Wide-gap emitters in heterojunction bipolar transistors (HBTs) allow a highly doped and therefore thinner base, reducing base transit time. Using wide-gap collectors results in double-HBTs (DHBTs) and offers the possibility of symmetric operation. All devices to be discussed here are of the n-p-n type.

AlGaAs/GaAs HBTs with emitter width of 1.2 μm have exhibited f(T) = 55 GHz and f(max) = 105 GHz; a ring oscillator with 14.2 ps

propagation delay per gate for 16.8 mW/gate has been demonstrated (IV,B6.1). HBTs with 30 nm base layers and epitaxial p^+-AlGaAs/p^+-GaAs embedded in the extrinsic base to make base contact have been reported (IV,B6.2). Self-aligned DHBTs with WSi_x/InAs/GaAs emitter contacts and p-AlGaAs barrier layers on the extrinsic-base surface for suppression of surface recombination have shown symmetric behavior, negligible offset voltage, and high current gains (IV,B6.3).

Replacing the GaAs base by a strained InGaAs layer has the advantages of lower growth temperature for InGaAs which reduces dopant diffusion, of higher carrier mobility, larger barrier, and reduced power dissipation. In particular, the splitting of the degeneracy of light and heavy hole bands in the strained InGaAs layer allows holes to populate preferentially the light hole bands, increasing hole mobility. AlGaAs/InGaAs/GaAs HBTs with $f(T) = 67$ GHz for 1.2×9 μm^2 emitter area have been demonstrated and a divide-by-four static frequency divider with an operating frequency as high as 20.1 GHz has been fabricated (IV,B6.4).

InGaAs/InP HBTs offer a higher minority carrier mobility, a reduced emitter-base voltage by suitable compositional grading, and a much lower surface recombination velocity than AlGaAs/GaAs HBTs. For InGaAs/InP DHBTs, the InP collector gives the additional advantage of superior high field drift velocity. All devices discussed in this material system are DHBTs. The low surface recombination makes the current gain independent of the emitter perimeter-to-area ratio and the first small area HBT in this material system has been reported (IV,B6.5) with a current gain of 275 and $f(T) = 18$ GHz for an emitter area of 5×10 μm^2 and a collector area of 2.9×10^{-6} cm^2. The first MOCVD grown InGaAs/InP HBTs, overcoming difficulties with Zn diffusion in InP, have been reported (IV,B6.6), (IV,B6.7), and give current gains as high as 5000 for 50 mA collector current (IV,B6.7).

The first InGaAs/InAlAs double heterojunction bipolar transistor (DHBT) has been demonstrated (IV,B3). Current gains in excess of 300 in emitter-up configuration were obtained.

IV,B6.1: M.-C. F. Chang, P. M. Asbeck, K. C. Wang, G. J. Sullivan, N.-H. Sheng, J. A. Higgins, and D. L. Miller, IEEE Electron Device Lett. EDL-8 (1987) 303

IV,B6.2: K. Taira, H. Kawai, and K. Kaneko, Electron. Lett. 23 (1987) 989

IV,B6.3: S. Tiwari and S. L. Wright, IEEE Electron Device Lett. EDL-8 (1987) 417

IV,B6.4: K. C. Wang, P. M. Asbeck, M. F. Chang, G. J. Sullivan, and D. L. Miller, IEEE Electron Device Lett. EDL-8 (1987) 383

IV,B6.5: R. N. Nottenburg, J.-C. Bischoff, M. B. Panish, and H. Temkin, IEEE Electron Device Lett. EDL-8 (1987) 282

IV,B6.6: P. A. Houston, C. Blaauw, A. Margittai, M. N. Svilans, N. Puetz, D. J. Day, F. R. Shepherd, and A. J. Springthorpe, Electron. Lett. 23 (1987) 931

IV,B6.7: J. R. Hayes, R. Bhat, H. Schumacher, and M. Koza, Electron. Lett. 23 (1987) 1298

IV.B.7. Hot Electron Transistors (HETs)

AlGaAs/GaAs HETs show common emitter gains up to 3.0 at 77°K, limited by scattering of the electrons into the L valleys in the GaAs base. For thin base layers (30 - 70 nm), bound and resonant states in the base well have been observed in tunneling hot-electron transfer amplifier (THETA) devices (IV,B7.1) as expected from quantum size effects.

A preferred base material is InGaAs, because of the larger Gamma-L energy separation and the higher electron velocity. InGaAs/InAlAs HETs on InP have been demonstrated (IV,B7.2), but gave poor current gains because of the high InAlAs collector barrier. For an InAlGaAs/InGaAs HET on InP with a collector barrier height of 0.27 eV, about half of that for InAlAs, a common-emitter current gain of 15.0 has been achieved at 77°K for a 25 nm thick base (IV,B7.3). The first InGaAs/InP HET has been reported (IV,B7.4).

Using a DBRT structure as emitter in a HET results in a resonant tunneling hot electron transistor (RHET) which exhibits novel functional characteristics due to the NDR of the DBRT structure.

A RHET with an InAlAs/InGaAs DBRT emitter, a 25 nm thick base, and an InAlGaAs collector on InP gave a common-emitter current gain of 28 at 77°K (IV,B7.5) which is five times the current gain of a corresponding AlGaAs/GaAs RHET.

IV,B7.1: M. Heiblum, M. V. Fischetti, W. P. Dumke, D. J. Frank, I. M. Anderson, C. M. Knoedler, and L. Osterling, Phys. Rev. Lett. 58 (1987) 816

IV,B7.2: U. K. Reddy, J. Chen, C. K. Peng, and H. Morkoc, Appl. Phys. Lett. 48 (1986) 1799

IV,B7.3: K. Imamura, S. Muto,, T. Fujii, N. Yokoyama, S. Hiyamizu, and A. Shibatomi, Electron Lett. 22 (1986) 1148

IV,B7.4: K. Ishihara, S. Kinoshita, K. Furuya, Y. Miyamoto, K. Uesaka, and M. Miyauchi, Japan. J. Appl. Phys. 26 (1987) L911

IV,B7.5: S. Hiyamizu, S. Muto, T. Inata, T. Fujii, K. Imamura, and N. Yokoyama, Third Internat. Conf. Superlattices, Microstructures & Microdevices, Chicago 1987, Program p. 67

IV.B.8. Charge Transfer Devices (CTDs)

Operation of an InP 64-bit charge coupled device (CCD) with 259 insulated gates has been reported by NOSC (IV,B8.1) to a measurement-limited upper frequency of 800 MHz. While GaAs is limited to single-level Schottky gate CCDs, the InP device has two levels of SiO_2 insulated transfer gates working in 4 phases, similar to Si NMOS technology. The charge transfer efficiency has been reported as greater than 0.998.

An interesting alternative to CCDs is acoustic charge transport (ACT) where charge packages are being transferred not by clocked gates, but by surface acoustic waves (IV,B8.2). ACT devices on GaAs are under development at various laboratories. ACT on InP has yet to be demonstrated.

IV,B8.1: L. Messick, D. A. Collins, and D. L. Lile, IEEE Electron Dev. Lett. EDL-7 (1986) 680

IV,B8.2: M. J. Hoskins, M. J. Brophy, J. M. Dallesasse, M. J. Miller, and J. W. Peterson, Proceed. 40th Annual Frequency Control Symposium 1986, Philadelphia, PA, p. 285

IV.C. Photonic Devices and Circuits

For reviews with emphasis on QW structures see (II,C.1) and (II,C.2). Recent reviews with emphasis on monolithic optoelectronic integrated circuits have been given by Forrest (IV,C.1) and Wada et al (IV,C.2).

IV,C.1: S. R. Forrest, J. Lightwave Technol. LT-3 (1985) 1248

IV,C.2: O. Wada, T. Sakurai, and T. Nakagami, IEEE J. Quantum Electronics QE-22 (1986) 805

IV.C.1. Photoemitters

Light emitting diodes (LEDs) have the advantage of low cost and high reliability over injection LDs (IV,C1.1), but exhibit lower performance. The upper modulation rate of LEDs is about 1 Gbit/s, an order of magnitude lower than LDs. Most of the present R&D aims at LDs with low threshold current J_{th} for laser action, low temperature sensitivity of the threshold current (IV,C1.2), stable single mode operation, and high modulation speed. The dependence of J_{th} on temperature T is of the form $\exp(T/T_o)$, hence a high value of the characteristic temperature T_0 is desired.

For GaAs lasers with cleaved mirrors, the photon density is limited by catastrophic damage of the cleaved mirror surfaces due to surface absorption. For InGaAsP lasers, the mirror damage threshold is at least an order of magnitude higher. For window and distributed feedback DFB laser structures, surface damage is not expected to be critical.

While buried-heterostructure (BH) lasers are highly developed, have very low J_{th}, and allow high modulation speed, they are difficult to fabricate which may make them incompatible with

high-yield monolithic integration. QW LDs are easier to fabricate than BH lasers. Compared to conventional double heterostructure lasers, the staircase shaped density of states leads to lower threshold currents, larger T_o, a reduced linewidth enhancement factor alpha (IV,C1.3), higher stability for single mode operation, reduced chirping, and less self-absorption in a lasing waveguide configuration; the stronger anisotropy of QW structures improves polarization stability which is particularly important for DFB LDs.

IV,C1.1: G.-K. Chang, H. P. Leblanc, and P. W. Shumate, Electron Lett. 23 (1987) 1338

IV,C1.2: M. M. Leopold, A. P. Specht, C. A. Zmudzinski, M. E. Givens, and J. J. Coleman, Appl. Phys. Lett. 50 (1987) 1403

IV,C1.3: L. D. Westbrook and M. J. Adams, Electron. Lett. 23 (1987) 1223

IV.C.1.a. **Visible Light**

For room temperature continuous wave (CW) operation of a transverse-mode stabilized AlGaInP LD on GaAs a power output of 27 mW has been obtained at a wavelength of 683 nm (IV,C1a.1); lasing down to 640 nm has been reported (IV,C1a.2) which is the shortest ever for room temperature CW operation of semiconductor LDs.

The first room temperature CW operation of a GaInP/AlGaInP MQW separate-confinement heterostructure (SCH) LD has been reported (IV,C1a.3) with an emission wavelength of 668 nm, a threshold current of 70 mA, and T_o = 138 K.

IV,C1a.1: H. Fujii, K. Kobayashi, S. Kawata, A. Gomyo, I. Hino, H. Hotta, and T. Suzuki, Electron. Lett. 23 (1987) 938

IV,C1a.2: S. Kawata, H. Fujii, K. Kobayashi, A. Gomyo, I. Hino, and T. Suzuki, Electron. Lett. 23 (1987) 1327

IV,C1a.3: M. Ikeda, A. Toda, K. Nakano, Y. Mori, and N. Watanabe, Appl. Phys. Lett. 50 (1987) 1033

IV.C.1.b. **Short Wavelength Near Infrared**

Most of the recently reported research on AlGaAs/GaAs LDs deals with QW structures. For an MBE grown graded-index (GRIN) separate-confinement heterostructure (SCH) SQW laser, a threshold current density of 93 A/cm^2 has been achieved (IV,C1b.1) which is almost a factor of 2 lower than the best previously reported figure. The same type of device, grown by MOCVD, gave a record external power efficiency of 55% with 1.5 W emitted power (IV,C1b.2). An array of separate-confinement DH SQW LDs had a threshold current of 45 mA and a total power conversion efficiency of 54% at a power output of 300 mW; the maximum CW power output, prior to catastrophic degradation of the output facet was 2 W for a 100 μm emitting aperture (IV,C1b.3). An output power of 10 W has been achieved for room temperature CW operation of a GaAs multi-stripe MQW laser (IV,C1b.4). Current modulation at 10 GHz has been reported for a MQW LD (IV,C1b.5), a factor of two higher than conventional DH LDs. Reduction of chirping by a factor of three has been observed (IV,C1b.6).

While the usual laser geometry is that of an edge emitter, face emission is desirable for multi-channel applications including free-space transmission. Surface emitting laser diodes (SELDs) also have advantages for MIOCs because cleaving is unnecessary. New approaches are SELDs with bent waveguides (IV,C1b.7) and grating coupled (GC) DFB SELDs (IV,C1b.8). An AlGaAs/GaAs bent DH SELD on a grooved substrate had a threshold current of 120 mA in pulsed operation with most of the light output between 5 and 45 degrees. For the AlGaAs/GaAs DFB transverse junction stripe (TJS) laser, the first room temperature CW lasing GC surface emission of 3 mW with diffraction limited 0.13 degree divergence has been demonstrated; the threshold current was 27 mA.

The first CW room temperature operation of a strained-layer InGaAs LD on GaAs has been reported (IV,C1b.9); the GRIN SCH SQW LD had a threshold current of 17 mA and gave 20 mW per facet for 80 mA near 1 μm. The first stimulated emission from ALE grown InAs/GaAs MQWs on GaAs with InAs wells as thin as 6.6 Å with 7.4% strain has been reported at 16^{o}K (IV,C1b.10).

IV,C1b.1: H. Z. Chen, A. Ghaffari, H. Morkoc, and A. Yariv, Electron. Lett. 23 (1987) 1334

IV,C1b.2: J. R. Shealy, Appl. Phys. Lett. 50 (1987) 1634

IV,C1b.3: D. F. Welch, M. Cardinal, W. Streifer, D. R. Scifres, and P. S. Cross, Electron. Lett. 23 (1987) 1240

IV,C1b.4: G. L. Harnagle, P. S. Cross, D. R. Scifres, and D. P. Worland, Electron. Lett. 22 (1986) 231

IV,C1b.5: K. Uomi, N. Chinoue, T. Otoshi, and T. Kajimura, Int. Symp. GaAs and Related Compounds, 1985, Inst. Phys. Conf. Ser. 79 (1986) 703

IV,C1b.6: N. K. Dutta, S. G. Napholtz, R. Yen, R. L. Brown, T. M. Shen, N. A. Olsson, and D. C. Craft, Appl. Phys. Lett. 46 (1985) 19

IV,C1b.7: M. Ogura, M.-C. Wu, W. Hsin, J. R. Whinnery, and S. Wang, Appl. Phys. Lett. 50 (1987) 705

IV,C1b.8: K. Mitsunaga, M. Kameya, K. Kojima, S. Noda, K. Kyuma, K. Hamanaka, and T. Nakayama, Appl. Phys. Lett. 50 (1987) 1788

IV,C1b.9: S. E. Fischer, D. Fekete, G. B. Feak, and J. M. Ballantyne, Appl. Phys. Lett. 50 (1987) 714

IV,C1b.10: M. A. Tischler, N. G. Anderson, R. M. Kolbas, and S. M. Bedair, Appl. Phys. Lett. 50 (1987) 1266

IV.C.1.c. Long Wavelength Near Infrared

A best-ever 22 GHz CW 3dB current modulation has recently been measured (IV,C1c.1) for an 1.3 μm InGaAsP/InP vapor-phase - regrown (VPR) BH laser. InGaAsP/InP semi-insulating planar buried heterostructure (SIPBH) LDs, using SI InP for current blocking have been demonstrated (IV,C1c.2); utilizing polyimide under

the bonding pads, a 3 dB response fall-off at 19 GHz has been obtained (IV,C1c.3) which is over twice the bandwidth obtained with other planar lasers.

For 1.5 - 1.6 μm dynamic single mode (DSM) operation with narrow dynamic spectral width (chirp), a new type of buried heterostructure (BH) bundle integrated guide (BIG) distributed Bragg reflector (DBR) laser (IV,C1c.4), and the first flat-surface BH (FBH) distributed feedback (DFB) lasers in this wavelength region (IV,C1c.5), (IV,C1c.6) have been demonstrated. For one of the FBH-DFB lasers, a threshold current of 9 mA, a bandwidth of 9.8 GHz, and a record single-longitudinal mode output power of 52 mW has been achieved (IV,C1c.5). For frequency modulation of a DFB LD, the advantages of a multi-electrode structure which allows adjustment of the current distribution has been demonstrated (IV,C1c.7).

A 1 mm by 3 mm two-dimensional array (incoherent) of 112 BH InGaAsP/InP SELDs with integrated beam deflectors has been demonstrated (IV,C1c.8) with a CW output of 14 mW per laser; an array optical flux of 57 W/cm^2 has been obtained when operating one section of the array; the total CW output of the array is thermally limited to 0.7 W.

To realize the theoretically expected superior performance of MQW LDs over DH LDs requires a high level of technology. In a comparison (IV,C1c.9) of InGaAs/InP DH and MQW LDs, threshold current densities of 1.3 and 1.5 KA/cm^2, and T_o of 35 - 45 and 65 - 80^{o}K, respectively, were obtained in pulsed operation. While these are the best results achieved for such lasers, the threshold current density of the MQW LD is still higher than for the DH LD. For an InGaAs/InGaAsP SCH MQW LD on InP with a threshold current of 18 mA, an output of 42 mW per facet and low internal loss has been reported (IV,C1c.10). For InGaAs/InAlAs on InP, the first CW room temperature operation of a MQW ILD has been reported with a threshold current of 530 mA and T_o = 62^{o}K (IV,C1c.11).

The best performance may be expected by combining QW structures with BH design, although the wells of subsequent structures were probably too thick to exhibit distinctive quantum effects. For an InGaAsP/InP real index guided double channel planar buried

heterostructure (DCPBH) DFB MQW LD, room temperature CW single mode operation at 1.3 μm with dynamic linewidth (chirp width) reduced by more than a factor of two compared to regular DH lasers has been reported (IV,C1c.12). The characteristic temperature has been increased from 60°K for regular DH lasers to 160 - 180°K for MQW lasers (IV,C1c.13), (IV,C1c.14).

Light emission from quantum-well boxes by current injection was observed for the first time for an InGaAsP/InP structure in pulsed operation at 77°K (IV,C1c.15) with the spectral fine structure suggesting stimulated emission.

IV,C1c.1: R. Olshansky, W. Powazinik, P. Hill, V. Lanzisera, and R. B. Lauer, Electron. Lett. 23 (1987) 839

IV,C1c.2: P. Speier, K. Wunstel, and F. J. Tegude, Electronic Lett. 23 (1987) 1363

IV,C1c.3: J. E. Bowers, U. Koren, B. I. Miller, C. Soccolich, and W. Y. Jan, Electron. Lett. 23 (1987) 1263

IV,C1c.4: I.-H. Choi, K. Komori, S. Arai, Y. Suematsu, K.-S. Lee, and M.-T. Pang, Japan. J. Appl. Phys. 26 (1987) L1593

IV,C1c.5: K. Kihara, K. Kamite, H. Sudo, T. Tanahashi, T. Kusunoki, S. Isozumi, H. Ishikawa, and H. Imai, Electron. Lett. 23 (1987) 941

IV,C1c.6: S. Nilsson, T. Tanbun-Ek, and B. Broberg, Appl. Phys. Lett. 51 (1987) 2082

IV,C1c.7: K. Iwashita, N. Takachio, Y. Nakano, and N. Tsuzuki, Electron. Lett. 23 (1987) 1022

IV,C1c.8: Z. L. Liau and J. N. Walpole, Appl. Phys. Lett. 50 (1987) 528

IV,C1c.9: W. T. Tsang, IEEE J. Quantum Electron. QE-23 (1987) 936

IV,C1c.10: U. Koren, B. I. Miller, Y. K. Su, T. L. Koch, and J. E. Bowers, Appl. Phys. Lett. 51 (1987) 1744

IV,C1c.11: Y. Matsushima, K. Utaka, K. Sakai, and O. Takeuchi, Electron. Lett. 23 (1987) 1271

IV,C1c.12: N. K. Dutta, S. G. Napholtz, A. B. Piccirilli, and G. Przybylek, Appl. Phys. Lett. 48 (1986) 1419

IV,C1c.13: N. K. Dutta, S. G. Napholtz, R. Yen, T. Wessel, T. M. Shen, and N. A. Olsson, Appl. Phys. Lett. 46 (1985) 1036

IV,C1c.14: Y. Sasai, N. Hase, M. Ogura, and T. Kajiwara, Int. Symp. GaAs and Related Compounds, Inst. Phys. Conf. Ser. 79 (1986) 709

IV,C1c.15: Y. Miyamoto, M. Cao, Y. Shingai, K. Furuya, Y. Suematsu, K. G. Ravikumar, and S. Arai, Japan. J. Appl. Phys. 26 (1987) L225

IV.C.1.d. Traveling-Wave Semiconductor Laser Amplifier (TWSLA)

The two types of semiconductor laser amplifiers for optical fiber transmission systems are Fabry-Perot amplifiers (FPAs) and traveling-wave amplifiers. Signal gain in FPAs is restricted to the vicinity of the resonance frequencies. TWSLAs have the advantage of wide gain bandwidth, theoretically in the order of THz, which assures stable amplifier operation in the face of deviations in amplifier temperature and optical input signal frequency, and they have superior signal gain saturation characteristics (IV,C1d.1).

Short wavelength NIR TWSLAs, based on AlGaAs/GaAs LDs, have been demonstrated in previous years. The first true TWSLA in the long wavelength NIR, based on InGaAsP LDs, was reported in 1987. The technological difficulty consists in reducing the facet reflectivity to the order of 0.01% by antireflection (AR) coating.

For 1.5 μm wavelength operation, near-traveling-wave operation has been reported from a BH LD with an internal cavity peak TE gain of 26.8 dB with a gain/wavelength ripple of 2.9 dB (IV,C1d.2). The first broadband true TWSLA at 1.5 μm has been

demonstrated by Nippon Telephone and Telegraph (NTT) with a gain/wavelength ripple of 1.5 dB for a 24.5 dB signal gain and a saturation output power of 7 dBm for a 20 dB signal gain (IV,C1d.1); a signal-spontaneous beat noise figure as low as 5.2 dB has been reported (IV,C1d.3). British Telecom Research Laboratories (BTRL) has used a DCPBH TWSLA as an optical repeater with 8 dB fiber-to-fiber gain in a 100 Mbit/s PSK heterodyne experiment (IV,C1d.4), as an optical preamplifier for a receiver resulting in a 3 dB bandwidth of 10 GHz with an electrical equivalent input noise as low as 1 $pA/Hz^{1/2}$ (IV,C1d.5), and for demonstration of a dynamic bandwidth of at least 50 GHz (IV,C1d.6).

For 1.3 μm operation, an InGaAsP channeled-substrate BH TWSLA with 13.1 dB fiber-to-fiber gain and 1 dB gain/wavelength ripple has been reported (IV,C1d.7).

As an alternative to AR coating, an 1.5 μm wavelength InGaAsP double-channel ridge-waveguide TWSLA with angled facets has been demonstrated (IV,C1d.8) with a gain/wavelength ripple of 2 dB for 19 dB signal gain. The residual modal reflectivity is estimated to be 0.2%. Combining angled facets and AR coating should vastly improve performance.

IV,C1d.1: T. Saitoh and T. Mukai, Electron. Lett. 23 (1987) 218

IV,C1d.2: J. C. Simon, B. Landousies, Y. Bossis, P. Doussiere, B. Fernier, and C. Padioleau, Electron. Lett. 23 (1987) 332

IV,C1d.3: T. Mukai and T. Saitoh, Electron. Lett. 23 (1987) 216

IV,C1d.4: R. C. Steele and I. W. Marshall, Electron. Lett. 23 (1987) 296

IV,C1d.5: I. W. Marshall and M. J. O'Mahony, Electron. Lett. 23 (1987) 1052

IV,C1d.6: I. W. Marshall, D. M. Spirit, and M. J. O'Mahony, Electron. Lett. 23 (1987) 818

IV,C1d.7: G. Eisenstein, B. C. Johnson, and G. Raybon, Electron. Lett. 23 (1987) 1020

IV,C1d.8: C. E. Zah, J. S. Osinski, C. Caneau, S. G. Menocal, L. A. Reith, J. Salzman, F. K. Shokoohi, and T. P. Lee, Electron. Lett. 23 (1987) 990

IV.C.1.e. Rare Earth Doped Laser Diodes

Rare earth (RE) doped semiconductor injection LDs, emitting not at the semiconductor bandgap but at a RE ion 4f-4f transition, may offer room temperature single mode operation without the use of distributed feedback, distributed Bragg reflectors, or external cavities.

Single mode CW room temperature operation of an erbium (Er) doped InGaAsP/InP LD has been demonstrated which emits at the Er^{3+} emission wavelength of 1.5322 μm (IV,C1e.1). The laser line shifted with temperature by 1 Å/K, which corresponds to that of a QW laser (IV,C1c.12), but is much less than the 6.5 Å/K for regular DH InGaAsP lasers. Alternatively, coherent emission in single mode pulsed operation of a similar LD has been attributed to inhomogeneities in the active layer resulting from Er doping and not to the Er levels (IV,C1e.2).

IV,C1e.1: W. T. Tsang and R. A. Logan, Appl. Phys. Lett. 49 (1986) 1686

IV,C1e.2: J. P. van der Ziel, M. G. Oberg, and R. A. Logan, Appl. Phys. Lett. 50 (1987) 1313

IV.C.2. Modulators

External optoelectronic modulation reduces chirp and eliminates partition noise which commonly limits the useful modulation rate of current modulated lasers. Modulation can be based either on electroabsorption (Franz-Keldysh effect) in bulk material, or on the QCSE of QW structures. For a BH InGaAs/InP modulator based on the Franz-Keldysh effect, an on/off ratio of 20 dB at 1.53 μm for an applied voltage of 8.5 V and a modulation bandwidth with 3 dB roll-off at 11 GHz have been reported (IV,C2.1).

The QCSE is the more efficient mechanism and gives less chirping due to a smaller linewidth broadening factor alpha. Modulators are usually built in waveguide configuration, with light propagation perpendicular to the applied electric field. AlGaAs/GaAs modulators have been demonstrated in the last few years; more recently, progress on InP based modulators has been reported.

For an InGaAs/InAlAs MQW modulator on InP, an on/off ratio of 20 dB at 1.53 μm has been achieved for an applied voltage as low as 2 V (IV,C2.2). The observed alpha of less than 1.0 is lower than that for a Franz-Keldysh modulator or an AlGaAs/GaAs MQW modulator.

InGaAs/InP MQW modulators are somewhat behind in development. A MOMBE grown modulator with an on/off ratio of 9 dB at 1.55 μm for 5 V applied bias has been reported (IV,C2.3). While intensity modulation desires a small value of alpha, phase modulation requires a large alpha. An InGaAs/InP MQW phase modulator with alpha up to 40 at 1.52 μm wavelength has been demonstrated and a half-wavelength shift has been achieved for 15 V bias voltage (IV,C2.4). In contrast, at 1.48 μm, the same device has an alpha of about 3 and acts as intensity modulator. MOCVD grown MQW intensity and phase modulators are under development at NOSC.

To achieve modulation at 1.3 μm, the InGaAs 2-D exciton energy can be moved into this wavelength region by making the QW thickness about 25 nm, but the QCSE becomes weak for such narrow wells. InGaAsP/InP QWs of appropriate alloy composition are more promising and QCSE in quaternary MQW structures has been demonstrated (IV,C2.5).

The first AlGaSb/GaSb MQW modulator has been reported (IV,C2.6) to give an on/off ratio of 10.5 dB at 1.55 μm with a 3 dB roll-off frequency of 3.7 GHz.

IV,C2.1: H. Soda, K. Nakai, H. Ishikawa, and H. Imai, Electron. Lett. 23 (1987) 1232

IV,C2.2: K Wakita, Y. Yoshikuni, M. Nakao, Y. Kawamura, and H. Asahi, Japan. J. Appl. Phys. 26 (1987) L1629

IV,C2.3: K Wakita, S. Nojima, K. Nakashima, and Y. Kawaguchi, Electron. Lett. 23 (1987) 1067

IV,C2.4: U. Koren, T. L. Koch, H. Presting, and B. I. Miller, Appl. Phys. Lett. 50 (1987) 368

IV,C2.5: H. Temkin, D. Gershoni, and M. B. Panish, Appl. Phys. Lett. 50 (1987) 1776

IV,C2.6: T. H. Wood, E. C. Carr, C. A. Burrus, R. S. Tucker, T.-H. Chiu, and W.-T. Tsang, Electron. Lett. 23 (1987) 540

IV.C.3. **Photodiodes**

Photodetectors allow simpler design than LDs because no waveguide structure is required. We shall discuss photovoltaic detectors and avalanche photodiodes (APDs). The first InGaAsP/InP heterojunction photodiodes (PDs) were reported by NOSC in 1977 (IV,C3.1), (IV,C3.2).

For the long-wavelength NIR, heterostructure InGaAs/InP APDs can have bit rates of several Gbit/s (IV,C3.3). The highest sensitivities are achieved with separate absorption, grading, and multiplication (SAGM) region APDs (IV,C3.4), where the InGaAs absorption and the InP multiplication regions are separated by one or more lattice-matched intermediate-bandgap InGaAsP layers; the observed pulse response time of 1.4 ns for a CBE grown device is limited by hole accumulation at the InP/InGaAsP interface. For an InGaAs/InP superlattice APD, a high speed response with full width at half-maximum (FWHM) of 200 ps has been measured (IV,C3.5). Reliability of APDs is a concern and degradation modes are under investigation (IV,C3.6).

Photovoltaic p-i-n diodes are easier to fabricate than APDs which makes them more useful for monolithic integration, they do not need the high bias of 60 V or more, and they are faster. InGaAs/InAlAs p-i-n photodiodes on SI InP with a rise time of 21 ps, a dark current of 1 nA, and a peak responsivity of 0.35 A/W have recently been reported (IV,C3.7). From the FWHM a 3-dB bandwidth of 18 GHz is estimated. The first InGaAs p-i-n

photodiode on Si for eventual monolithic integration with Si ICs has been demonstrated (III,A.24).

For mid-IR FO at 2.55 μm wavelength, a compositionally graded InGaAs detector on InP substrate has been reported (IV,C3.8). A data transmission experiment at 2.4 μm wavelength gave at 34 Mbit/s an extrapolated receiver sensitivity of -31.5 dBm for 10^{-9} BER. An alternate detector approach, InGaAsSb on InAs or GaSb substrates, has been under investigation at NOSC.

IV,C3.1: H. H. Wieder, A. R. Clawson, and G. E. McWilliams, Appl. Phys. Lett. 31 (1977) 468

IV,C3.2: A. R. Clawson, W. Y. Lum, G. E. Mc Williams, and H. H. Wieder, Appl. Phys. Lett. 32 (1978) 549

IV,C3.3: S. R. Forrest, J. Lightwave Technol. LT-2 (1984) 34

IV,C3.4: W.-T. Tsang, J. C. Campbell, and G. J. Qua, IEEE Electron Device Lett. EDL-8 (1987) 294

IV,C3.5: F. Beltram, J. Allam, F. Capasso, U. Koren, and B. Miller, Appl. Phys. Lett. 50 (1987) 1170

IV,C3.6: H. Sudo, M. Suzuki, and N. Miyahara, IEEE Electron Device Lett. EDL-8 (1987) 386

IV,C3.7: Y. Zebda, P. Bhattacharya, M. S. Tobin, and T. B. Simpson, IEEE Electron Device Lett. EDL-8 (1987) 579

IV,C3.8: R. A. Garnham, D. G. Cunningham, and W. A. Stallard, Electron. Lett. 23 (1987) 1063

IV.C.4. Photoconductive Switches

Photoconductive detectors with high off-resistance, low on-resistance, and short time constants, illuminated with ps pulses, serve as optoelectronic switches. To obtain a high off-resistance, semi-insulating materials are preferred such as SI InP, GaAs, or InGaAs. A short turn-off time constant can be achieved by fast carrier recombination and sweep-out.

Recombination rates in SI materials are high and can be further enhanced by proton or ion bombardment. Carrier sweep-out depends on the applied bias, but because of carrier screening may not be as effective as expected (IV,C4.1). Applications include high-speed sampling and RF mixing. A review has been provided by Foyt and Leonberger (IV,C4.2).

Semi-insulating Fe doped InP switches are under development at NOSC. For Ti doped SI InP switches, off-resistance of about 100 MOhm, comparable to that of Fe doped devices, on-resistance of about 4°KOhm, which is 10 times lower than that of Fe doped devices, and pulse response times of 60 ps FWHM, comparable to proton-bombarded InP:Fe devices have been observed (IV,C4.3).

A response time of 19 ps was reported for GaAs-on-SOS switches (IV,C4.1). Fe doped InGaAs switches were considerably slower, with the response times depending on the size of the device and the applied bias, reaching about 100 ps (IV,C4.1).

For an interdigitated coplanar proton-bombarded GaAs switch integrated on GaAs substrate, a FWHM switching time of 7 ps has been achieved (IV,C4.4).

A tandem IC of InP switches which allows variations of electric pulses between 40 and 400 ps FWHM has been reported (IV,C4.5).

A 4:1 time-division multiplexer using Cr doped GaAs switches activated by a GaAs laser with optical fiber delay lines has been demonstrated at NOSC (IV,C4.6) at 2.5 Gbit/s for potential application to VLSI off-chip data transmission.

With contacts shaped as antennas, photoconductive switches can be used for mm-wave generation and detection. The response of tapered slot antennas on oxygen-ion-bombarded Si has been investigated (IV,C4.7).

IV,C4.1: E. A. Chauchard, C. H. Lee, V. Diadiuk, and G. W. Turner, Picosecond Electronics and Optoelectronics, 1987 Technical Digest Series, Optical Society of America, Vol. 1, p. 89

IV,C4.2: A. G. Foyt and F. J. Leonberger, in Picosecond Optoelectronic Devices, ed. by C. H. Lee, Academic Press, New York, 1983

IV,C4.3: V. Diadiuk, G. W. Iseler, G. A. Ferrante, and C. H. Cox, IEEE Trans. Electron Devices ED-33 (1986) 1862

IV,C4.4: H. Schumacher, U. Salz, and H. Beneking, Picosecond Electronics and Optoelectronics, 1987 Technical Digest Series, Optical Society of America, Vol. 1, p. 82

IV,C4.5: Y. Hori, J. Palaski, M. Yi, and A. Yariv, Appl. Phys. Lett. 46 (1985) 750

IV,C4.6: D. J. Albares, G. A. Garcia, C. T. Chang, and R. E. Reedy, Electron. Lett. 23 (1987) 327

IV,C4.7: A. P. DeFonzo, C. R. Lutz, and M. Jarwala, Picosecond Electronics and Optoelectronics, 1987 Technical Digest Series, Optical Society of America, Vol. 1, p. 40

IV.C.5. **Solar Cells**

AlGaAs/GaAs solar cells with areas of 2 x 2 cm^2 have shown conversion efficiencies of 21% under one sun, air mass zero (AM0) conditions both for p-n and n-p configurations (IV,C5.1). InP solar cells are of interest for space applications because of their superior radiation hardness (II,B.11), (II,B.12) compared to GaAs or Si; n^+-p homojunction cells with a conversion efficiency of 13 to 14% under AM0 illumination and 16.5% for AM1.5 have been demonstrated (IV,C5.2). More recently, higher conversion efficiencies of 17.2% for AM0 and 21.5% for AM1.5 illumination have been reported for InP p^+-i-n solar cells (IV,C5.3), but their radiation hardness is lower than that of the InP n^+-p cells because electron irradiation introduces recombination centers in the i-layer.

For absorption of an AM0 spectrum, the optimum bandgap is about 1.5 to 1.6 eV. This is larger than that of InP and GaAs, but can be achieved with quaternary alloys. An indium tin oxide (ITO)/InGaAsP solar cell lattice matched to GaAs with a bandgap

of 1.55 eV of the quaternary alloy has shown a conversion efficiency of 9.6% under AM1 illumination without antireflection coating (IV,C5.4). This is not as good as expected, compared to a previously reported ITO/InP heterojunction solar cell (IV,C5.5) which gave a total area conversion efficiency of 16.2% for AM1.5 illumination, corresponding to an active area efficiency of 19.1%.

IV,C5.1: J. G. Werthen, G. F. Virshup, C. W. Ford, C. P. Lewis, and H. C. Hamaker, Appl. Phys. Lett. 48 (1986) 74

IV,C5.2: A. Yamamoto, M. Yamaguchi, and C. Uemura, Appl. Phys. Lett. 44 (1984) 611

IV,C5.3: Y. Itoh, M. Yamaguchi, and C. Uemura, IEEE Electron Device Lett. EDL-7 (1986) 127

IV,C5.4: H. Narui, S. Matsubara, N. S. Takahashi, and S. Kurita, Japan. J. Appl. Phys. 26 (1987) L91

IV,C5.5: T. J. Coutts and S. Naseem, Appl. Phys. Lett. 46 (1985) 164

IV.C.6. **Novel Device Functions**

A DH InGaAsP/InP unstable resonator LD with wet-etched curved facets has been demonstrated (IV,C6.1). This geometry suppresses filamentation and promises improved focusing properties. An output power of 105 mW from each facet was measured.

The first optical polarization bistability has been observed in an 1.3 μm wavelength InGaAsP/InP BH LD between the transverse electric (TE) and the transverse magnetic (TM) mode, induced by injection of the TM wave (IV,C6.2). The bistability is probably of the dispersive type, caused by gain interaction. Switching speed is 200 ps up and 430 ps down.

Chemla (II,C.2) and Okamoto (II,C.3) describe a variety of novel QW devices and functions based on the QCSE, the 2-D exciton optical nonlinearity, and the self-electro-optic device (SEED).

Devices of the QW modulator type based on the QCSE have been discussed in Section IV.C.2.

Optical switching and bistability at 1.55 μm wavelength in Fabry-Perot MQW etalons has been observed in InGaAs/InP at 77^{o}K (IV,C6.3) and in InGaAs/InAlAs at room temperature (IV,C6.4). These devices have promise for all-optical logic operations.

Carrier induced bleaching in SQW MODFETs has been investigated for AlGaAs/GaAs (IV,C6.5) and for InAlAs/InGaAs on InP (IV,C6.6) with the carrier density controlled by the FET gate bias. A FET optical modulator (FETOM) promises high speed, small size, and low power consumption for optoelectronic integration (IV,C6.7), (IV,C6.8); related proposed devices are an optically readable memory element and an optically switched charge storage device.

While the nonlinear phenomena displayed by present QW devices are caused by real charge carriers, much faster effects, in the picosecond or even sub-ps range, may be expected for all-optical bistable or logic elements from the optical Stark effect (II,C.11), (II,C.13), or from screening by virtual charge carriers (II,C.14), (II,C.15) as briefly discussed in Section II,C.

IV,C6.1: H. Wang, Y. Y. Liu,, M. Mittelstein, T. R. Chen, and A. Yariv, Electron. Lett. 23 (1987) 949

IV,C6.2: Y. Mori, J. Shibata, and T. Kajiwara, Appl. Phys. Lett. 51 (1987) 1971

IV,C6.3: K. Tai, J. L. Jewell, W. T. Tsang, H. Temkin, M. Panish, and Y. Twu, Appl. Phys. Lett. 50 (1987) 795

IV,C6.4: H. Kawaguchi and Y. Kawamura, Electron Lett. 23 (1987) 1013

IV,C6.5: H. Sakaki, H. Yoshimura, and T. Matsusue, Japan. J. Appl. Phys. 26 (1987) L1104

IV,C6.6: D. S. Chemla, I. Bar-Joseph, C. Klingshirn, D. A. B. Miller, J. M. Kuo, and T. Y. Chang, Appl. Phys. Lett. 50 (1987) 585

IV,C6.7: A. Kastalsky, J. H. Abeles, and R. F. Leheny, Appl. Phys. Lett. 50 (1987) 708

IV,C6.8: J. H. Abeles, A. Kastalsky, and R. F. Leheny, J. Lightwave Technol. LT-5 (1987) 1296

IV.D. Integrated Optoelectronic Circuits

Monolithic optoelectronic integrated circuits (MOICs) offer functionality and performance (speed, noise) improvements over hybrid circuits by reduction of parasitics, require less components allowing for easier assembly, are more compact and of lower weight, give higher reliability, and result in reduced costs if produced in sufficient numbers. MIOCs have the disadvantage that they require high material quality to give acceptable yield, it is technologically difficult to optimize all of the integrated devices simultaneously, the requirement of different material layers may result in surface steps of several μm which complicates processing, undesirable device interactions may occur, and heat removal may be a problem.

Applications include fiber optics communications, optical interconnects within and between high speed large scale integration (LSI) chips and boards, and arrays of individually addressable photoemitters or photodetectors for optical processing, optical computation, and computer interconnections. The first transmission experiments with packaged MIOC transmitter and receiver modules for local area networks (LANs) have been demonstrated for 400 and 800 Mbit/s over 4 and 2 km, respectively, at 10^{-9} BER (IV,D.1). Presently, MIOCs do not meet the theoretical expectations, but perform usually worse than hybrid circuits presumably due to technological difficulties.

InP based MIOCs, compared to GaAs, have the advantage that the substrate is transparent for the wavelengths employed. This allows back illumination for detectors and largely eliminates optical cross talk between lasers and transistors which can degrade device performance in AlGaAs/GaAs MIOCs. InP based MIOCs will also benefit from the potentially higher speed of the electronic devices to be integrated, compared to GaAs. The disadvantage is the less advanced state of InP based technology

and, related to that, the higher costs. This is aggravated by the fact that for the dominating commercial application, FO communications, long distance InP based transmission systems which would profit most from integration represent less of a volume market than short distance GaAs based systems.

Reviews of MIOC development have been presented by Yariv (IV,D.2), by Forrest (IV,C.1), and by Wada et al (IV,C.2).

IV,D.1: T. Horimatsu, T. Iwama, Y. Oikawa, T. Touge, M. Makiuchi, O. Wada, and T. Nakagami, J. Lightwave Technol. LT-4 (1986) 680

IV,D.2: A. Yariv, IEEE Trans. Electron Devices ED-31 (1984) 1656

IV.D.1. Photoemitter Integration

For integration, laser diodes are preferred over LEDs to exploit the available speed potential. Various examples of monolithic integration of GaAs QW lasers with GaAs MESFET driver circuits, input buffers, multiplexers, etc, are presented in (IV,C.1) and (IV,C.2). Typically, modulation rates of 2 Gbit/s are obtained with the speed of the response limited by the LD, not the electronic circuit. Photodiodes have been integrated either for laser monitoring or to demonstrate optical repeaters. For a packaged transmitter module a bandwidth of 1.65 GHz has been obtained (IV,D.1).

Horizontal integration of LDs and HBTs in InGaAsP/InP technology is in progress. Vertical integration of a LD and a HBT has recently been reported (IV,D1.1), allowing base current controlled laser operation and novel device functions (see Section IV.D.4).

LED and laser arrays represent a different type of integration. Examples of GaAs and InP based arrays are discussed in (IV,C.1). The first operation of a phase-locked InGaAs/InP laser arrays emitting at 1.3 μm has been demonstrated for ridge island LDs (IV,D1.2). Output powers greater than 300 mW pulsed and 120 mW CW have been obtained without facet coatings.

IV,D1.1: T. R. Chen, K. Utaka, Y. H. Zhuang, Y. Y. Liu, and A. Yariv, Appl. Phys. Lett. 50 (1987) 874

IV,D1.2: M. Razhegi, R. Blondeau, M. Krakowski, B. de Cremoux, J. P. Duchemin, F. Lozes, M. Martinot, and M. A. Bensoussan, Appl. Phys. Lett. 50 (1987) 230

IV.D.2. Modulator Integration

The first integration of a GaAs directional-coupler waveguide modulator, based on the linear electro-optic effect, with GaAs power MESFETs gave an electro-optic figure-of-merit superior to that for $LiNbO_3$ (IV,D2.1).

A 2 x 2 optical gate matrix switch has been demonstrated which monolithically integrates AlGaAs/GaAs MQW modulators with miniaturized optical splitters and combiners (IV,D2.2).

Monolithic integration of an InGaAs/InAlAs MQW modulator with a 1.556 μm wavelength InGaAsP DFB LD has shown a 55% depth of modulation for a modulator reverse bias voltage of 5 V, and a rise time of the light output response of 300 ps limited by the RC time constant of the modulator (IV,D2.3). At present, the modulation efficiency is not as high as that obtained with a discrete MQW modulator.

IV,D2.1: J. H. Abeles, W. K. Chan, F. K. Shokoohi, R. Bhat, and M. A. Koza, Electron. Lett. 23 (1987) 1037

IV,D2.2: A. Ajisawa, M. Fujiwara, J. Shimizu, M. Sugimoto, M. Uchida, and Y. Ohta, Electron. Lett. 23 (1987) 1121

IV,D2.3: Y. Kawamura, K. Wakita, Y. Yoshikuni, Y. Itaya, and H. Asahi, IEEE J. Quantum Electron. QE-23 (1987) 915

IV.D.3. Photodetector Integration

Monolithic integration lends itself to reduce the receiver front-end capacitance by reducing the detector diameter which increases

receiver speed. Various examples of IR receiver front-ends by integration of GaAs p-i-n PDs with FET preamplifiers (PIN-Amps) or of InGaAs p-i-n PDs with InP MISFETs, InP JFETs, or InGaAs JFETs are presented in (IV,C.1) and (IV,C.2). Present monolithic receivers perform worse than their hybrid counterparts, probably due to parasitic interactions on the chip. It is expected that improvements in material and device technologies and in design will lead to full realization of the performance potential of monolithic photoreceivers.

A packaged GaAs PIN-Amp receiver module (IV,D.1) had a bandwidth of 360 MHz limited by the PD capacitance; receiver sensitivity was -20.6 dBm at 400 Mbit/s and -18.4 dBm at 800 Mbit/s for 10^{-9} BER. This performance is considerably inferior to hybrid receivers.

Compared to GaAs, much less work has been done on monolithic InP based receivers, although it is in the long-wavelength region where the greatest advantages are expected from integration. A monolithic PIN-FET consisting of a selectively grown InGaAs p-i-n detector and an InP D-MISFET on SI InP substrate had a sensitivity of -34 dBm at 90 Mbit/s and -29.5 dBm at 295 Mbit/s NRZ for 10^{-9} BER (IV,D3.1). An InGaAs PIN-FET on InP substrate with a sensitivity of -33.7 dBm at 140 Mbit/s for 10^{-9} BER has been demonstrated (IV,D3.2). A monolithic PIN-Amp receiver front-end consisting of a p-i-n InGaAs detector and an InP JFET preamplifier is under development at NOSC in cooperation with the University of Southern California (USC).

A hybrid receiver for 1.3 and 1.55 μm has been reported (IV,D3.3), consisting of a commercial InGaAs PIN PD and a three-stage GaAs FET preamplifier. The receiver has a 3 dB bandwidth of 8 GHz and an electrical equivalent input noise of less than 12 $pA/Hz^{1/2}$ from 4 - 7 GHz. Notice that this equivalent noise, while quite good compared to conventional receivers, is an order of magnitude higher than what can be achieved with a TWSLA (IV,C1d.5).

The first GaAs-on-InP strained-layer PIN-FET, obtained by integration of an InGaAs PD with a GaAs MESFET on InP substrate has a sensitivity of -31 dBm for 600 Mbit/s NRZ random optical signals at 10^{-9} BER (III.A.19).

The first InGaAs-on-GaAs strained-layer monolithic photoreceiver, grown by low pressure MOCVD, has been reported (III,A.16), consisting of a 1.3 - 1.55 μm wavelength $In_{0.53}Ga_{0.47}As$ photoconductive detector and a GaAs MESFET.

Monolithic integration of an InGaAs/InP p-i-n photodiode with an InP (IV,D3.4) and an InAlGaAs (IV,D3.5) waveguide has been reported.

IV,D3.1: B. Tell, A. S. H. Liao, K. F. Brown-Goebeler, T. J. Bridges, G. Burckhardt, T. Y. Chang, and N. S. Bergano, IEEE Trans. Electron Devices ED-32 (1985) 2319

IV,D3.2: J. C. Renaud, L. N'Guyen, M. Allovon, F. Heliot, F. Lugiez, and A. Scavennec, Electron. Lett. 23 (1987) 1055

IV,D3.3: J. L. Gimlett, Electron. Lett. 23 (1987) 281

IV,D3.4: S. Chandrasekhar, J. C. Campbell, A. G. Dentai, C. H. Joyner, G. J. Qua, and W. W. Snell, IEEE Electron Device Lett. EDL-8 (1987) 512

IV,D3.5: P. Cinguino, F. Genova, C. Rigo, C. Cacciatore, and A. Stano, Appl. Phys. Lett. 50 (1987) 1515

IV.D.4. Novel Integrated Structures

New functions have been demonstrated, based on the nonlinearities resulting from the interaction of vertically integrated electronic and photonic structures.

The double heterostructure optoelectronic switching device (DOES) (IV,D4.1) may be considered a vertical integration of a n-AlGaAs/n-GaAs open-source bipolar inversion channel field effect transistor (BICFET) with a n-GaAs/p^+-AlGaAs LED or laser diode. The BICFET has a 3 - 4 nm p-doped layer at the n-n heterointerface, and the integrated structures share the active n-GaAs layer. The device has binary electrical and binary optical states that may be changed either by an electrical or an optical input. Operated as an electrical switch and biased as a relaxation oscillator, a turn-on speed of 100 ps was measured,

while the turn-off speed was limited by the RC pull-up time (IV,D4.2). The expected true switching time is estimated as 2 ps.

Vertical integration of an InGaAsP/InP DH mass transport LD with an InGaAsP/InP DHBT gives an p-n-p-n structure with thyristor-like I-V characteristics allowing operation as an electro-optic bistable laser or an electro-optical switching laser (IV,D1.1).

The first monolithic optoelectronic logic device (OELD) has been demonstrated (IV,D4.3) in AlGaAs/GaAs technology by vertical integration of an n-p-n bipolar heterojunction phototransistor with a MQW QCSE modulator, resulting in SEED-like operation for potential use in digital processing systems.

A 2 x 2 array of optically bistable switches consisting of AlGaAs/GaAs SEED structures obtained by vertical integration of a MQW p-i-n PD with a load photodiode has been demonstrated (IV,D4.4). Optical control power can vary between 40 pW and 470 W with associated switching times of 10 s and 2 s.

IV,D4.1: J. G. Simmons and G. W. Taylor, IEEE Trans. Electron Devices ED-34 (1987) 973

IV,D4.2: G. W. Taylor, J. G. Simmons, R. S. Mand, and A. Y. Cho, IEEE. Trans Electron Devices ED-34 (1987) 961

IV,D4.3: P. Wheatley, G. Parry, J. E. Midwinter, G. Hill, P. Mistry, M. A. Pate, and J. S. Roberts, Electron. Lett. 23 (1987) 1249

IV,D4.4: D. A. B. Miller, J. E. Henry, A. C. Gossard, and J. H. English, Appl. Phys. Lett. 49 (1986) 821

V. SUMMARY AND RECOMMENDATIONS

In spite of the immature state of InP based technology, devices usually outperform their GaAs counterparts wherever equivalent structures exist. InP is superior to GaAs as far as electron peak velocity, NDR of the velocity-field characteristics, electric breakdown, side-gating, radiation hardness, and thermal

conductivity are concerned. This makes InP of interest for power devices, Gunn diodes, and solar cells for space applications, but also suggests the development of InP JFET ICs with improved radiation hardness over GaAs MESFETs or JFETs and reduced side-gating which is expected to limit the packing density of GaAs ICs. Submicron gate length is more difficult to achieve for JFETs than for MESFETs, but the speeds achievable with n-channel technology should allow a wide range of applications. While holes are slow in InP, the feasibility of complementary JFET ICs should be investigated as it is done for GaAs.

For high speed applications, InGaAs lattice-matched to InP is the preferred active material, both for horizontal type devices such as MISFETs, JFETs, HIGFETs, and MODFETs, as well as for vertical devices such as HBTs, HETs, and double-barrier resonant-tunneling structures. InGaAs, however, does not have the high electric breakdown strength of InP and may not have the high resistance to irradiation and side-gating.

It is a fortunate coincidence that the superior properties of silica fibers at 1.3 and 1.55 μm wavelength can be covered by the bandgaps of InP based alloys for photonic components. Independent of FO applications, the combination of the high speed of InP based electronic devices with the transparency of InP at these wavelengths promises superior MOICs compared to GaAs. It would be a mistake to rely on industry to lead the development of InP MOICs for FO, because the volume market is in short-distance GaAs based FO, not in the long distance InP based FO applications. While present hybrid optoelectronic circuits perform better than their monolithic counterparts, this should change with improvements in technological capabilities and should lead to MIOCs with superior performance and reliability and, eventually, to reduced cost.

For practically every electronic and photonic device type that allows a 2-DEG or QW version, this version offers or promises performance superior to the conventional design. In addition, QW structures are frequently less complicated in design and therefore easier to integrate, and they offer functions not available conventionally. This means that semiconductor electronics for the next decades will be dominated by QW devices and ICs.

In technology, starting with substrates, InP bulk material needs to be improved. Quality improvement is in progress by magnetic field LEC, the VGF method, and other techniques. Cost reductions, compared to the present two-step growth techniques, may result from direct synthesis using gaseous or liquid P.

In epitaxy, both MOCVD and various types of MBE allow the growth of high quality InP based materials and of abrupt heterojunctions, but further improvements in the starting materials and in epitaxial methods are needed. Pseudomorphic growth is of scientific and technical significance, but the possibilities of InP-on-Si or InP-on-GaAs should not be used as an excuse to neglect the development of InP substrates. For active InGaAs layers the preferred choice for high speed and stability should be lattice matched growth, unless required otherwise for special reasons.

Current drift in InP and InGaAs MIS structures requires prudent choice of applications for this technology. For InP power MISFETs, the gate RF bias seems to alleviate drift and the combination of insulated gate and superior electrical properties of InP gives device performance superior to GaAs power MESFETs. If the problem of insulators on III-V compounds finds a general solution, such as intermediate pseudomorphic growth of a few monolayers of Si, this would allow a GaAs MISFET technology. Nevertheless, InP would remain superior for power applications, InGaAs for speed, and InP JFETs for radiation hardness and reduced side-gating.

To take advantage of the opportunities promised by InP and InGaAs technology, broad Government support will be required. Many of the features offered, such as extreme speed, high power, and radiation hardness, are primarily of interest to the military and will not be accomplished by industry without major DoD support.

Index

Glossary

1-D (one dimensional)
2-D (two-dimensional)
3-D (three-dimensional)
2-DEG (two-dimensional electron gas)
ACT (acoustic charge transport)
AlAs (aluminum arsenide)
ALE (atomic layer epitaxy)
AlGaAs (aluminum gallium arsenide)
AlGaSb (aluminum gallium antimonide)
AM0 (air mass (zero))
APD (avalanche photodiode)
AR (antireflection)
BER (bit error rate)
BH (buried heterojunction or buried heterostructure)
BICFET (bipolar inversion channel FET)
BIFET (buried interface FET)
BIG (bundle integrated guide)
BTRL (British Telecom Research Laboratories)
CAIBE (chemically assisted ion beam etching)
CBD (chemical beam epitaxy)
CBE (chemical beam epitaxy)
CBM (conduction band minimum)
CCD (charge-coupled device)
Cd (cadmium)
Co (cobalt)
Cr (chromium)
CTD (charge transfer device)
CW (continuous wave)
DARPA (Defense Advanced Research Projects Agency)
DBD (double barrier diode)
DBR (distributed Bragg reflector (laser diode)
DBRT (double barrier resonant-tunneling)
DCFL (direct coupled FET logic)
DCPBH (double channel planar buried heterostructure)
DFB (distributed feedback (laser diodes))
DHBT (double heterojunction bipolar transistor)
DHSELD (double heterostructure surface emitting laser diode)
D-MESFET (depletion metal-semiconductor-field-effect-transistor)
D-MISFET (depletion-metal-insulator-semiconductor-field-effect-transistor)
DMT (doped channel MIS-like FET)
D-MISFET (depletion metal-insulator-semiconductor field effect transistor)
DOES (double-heterostructure optoelectronic switching device)
DSM (dynamic single mode)
E/D (enhancement/depletion)
E-JFET (enhancement JFET)
E-MISFET (enhancement MISFET)
EPD (etch pit density)
Er (erbium)
FBH (flat-surface buried heterostructure (laser diode))
Fe (iron)
FET (field effect transistor)
FETOM (field effect transistor optical modulator)
FIB (focused ion beam)
FO (fiber optic)
FPA (focal plane array or Fabry-Perot amplifier)
FWHM (full-width at half-maximum)
GaAs (gallium arsenide)
GaSb (gallium antimonide)
GC (grating coupled)
GRIN (graded-index)
GSMBE (gas source molecular beam epitaxy)
HBT (heterojunction bipolar transistor or heterostructure bipolar transistor)
HEMT (high electron mobility transistor)
HET (hot electron transistor)
HgCdTe (mercury cadmium telluride)
HIFET (hetero-interface FET)
HIGFET (heterojunction insulated gate FET)
IC (integrated circuit)
InAlAs (indium aluminum arsenide)
InAs (indium arsenide)
InGaAsP (indium gallium

arsenide phosphide)
InP (indium phosphide)
ILD (integrated laser diode)
IMPATT (impact ionization avalanche transit time diode)
IOC (integrated optoelectronic circuit)
IOEC (integrated optoelectronic circuit)
IR (infrared)
IRFPA (infrared focal plane array)
ITO (indium tin oxide)
JFET (junction field effect transistor)
LAN (local area network)
LD (laser diode)
LEC (liquid encapsulated Czochralski)
LED (light emitting diode)
LPCZ (liquid-phosphorus encapsulated Czochralski)
LPE (liquid phase epitaxy)
LPMOCVD (low pressure metalorganic chemical vapor deposition)
LSI (large scale integration)
MAD (multiple-acronym device)
MBE (molecular beam epitaxy)
MEE (migration-enhanced epitaxy)
MESFET (metal-semiconductor field effect transistor)
MIBE (molecular/ion beam epitaxy)
MIMIC (microwave/millimeterwave monolithic integrated circuit)
MIOC (monolithic integrated optoelectronic circuit)
MIS (metal-insulator-semiconductor)
MISFET (metal-insulator-semiconductor FET)
MLEC (magnetic liquid-encapsulated Czochralski)
MMIC (monolithic microwave integrated circuit)
MOIC (monolithic optoelectronic integrated circuit)
MOCVD (metalorganic chemical vapor deposition)
MODFET (modulation-doped FET)
MOMBE (metalorganic molecular beam epitaxy)
MOS (metal-oxide-semiconductor)
MOSFET (metal-oxide-semiconductor FET)
MQW (multiple quantum-well)
NDR (negative differential resistance)
NEC (Nippon Electric Company)
NIR (near infrared)
NMOS (n-channel metal-oxide-semiconductor)
NOSC (Naval Ocean Systems Center)
NRL (Naval Research Laboratory)
NRZ (non-return to zero)
N_{SS} (surface state density)
NTT (Nippon Telephone and Telegraph)
OELD (optoelectronic logic device)
OMVPE (organometallic vapor phase epitaxy)
ONT (Office of Naval Technology)
PAE (power added efficiency)
PBT (permeable base transistor)
PD (photodetector or photodiode)
PECVD (plasma-enhanced chemical vapor deposition)
PIN-Amp (p-i-n photodetector monolithically integrated with amplifier)
PIN-FET (p-i-n photodetector monolithically integrated with FET)
QCSE (quantum-confined Stark effect)
QW (quantum-well)
QWITT (quantum-well injection transit-time)
RCA (Radio Corporation of America)
RE (rare earth)
RF (radio frequency)
RHET (resonant tunneling hot electron transistor)
RT (resonant tunneling)
RTB (resonant tunneling barrier)
S (sulfur)
SAGM (separate absorption, grating and multiplication (photodiode))

SCH (separate-confinement heterostructure)
SCHILD (separate-confinement heterostructure injection laser diode)
SDHT (selectively doped heterostructure transistor)
SEED (self-electro-optic device)
SELD (surface emitting laser diode)
Si (silicon)
SI (semi-insulating)
SIPBH (semi-insulating planar buried heterostructure)
SISFET (semiconductor-insulator-semiconductor FET)
SL (superlattice)
SLS (strained-layer superlattice)
SOI (silicon-on-insulator or semiconductor-on-insulator)
SOS (silicon-on-sapphire)
SQW (single quantum-well)
SRAM (static random access memory)
TE (transverse electric)
TED (transferred electron device)
TEGFET (two-dimensional electron gas FET)
THETA (tunneling hot-electron transfer amplifier)
Ti (titanium)
TJS (transverse junction stripe (laser diode))
TM (transverse magnetic)
TWSLA (traveling wave semiconductor laser amplifier)
UCSD (University of California, San Diego)
UHV (ultra high vacuum)
USC (University of Southern California)
VCE (vacuum chemical epitaxy)
VFET (vertical field effect transistor)
VGF (vertical gradient freeze)
VMOS (vertical MOS)
VPE (vapor phase epitaxy)
VPR (vapor phase regrown (laser diode))
WN (tungsten nitride)
WSi (tungsten silicide)
Yb (ytterbium)
Zn (zinc)